



Structural, lithological, and geodynamic controls on geothermal activity in the Menderes geothermal Province (Western Anatolia, Turkey)

Vincent Roche¹ · Vincent Bouchot¹ · Laurent Beccaletto¹ · Laurent Jolivet² · Laurent Guillou-Frottier¹ · Johann Tuduri¹ · Erdin Bozkurt^{3,4} · Kerem Oguz⁵ · Bülent Tokay³

Received: 7 February 2018 / Accepted: 26 September 2018 / Published online: 8 October 2018
© Springer-Verlag GmbH Germany, part of Springer Nature 2018

Abstract

Western Turkey belongs to the regions with the highest geothermal potential in the world, resulting in significant electricity production from geothermal resources located predominantly in the Menderes Massif. Although geothermal exploitation is increasingly ongoing, geological, and physical processes leading to the emplacement of geothermal reservoirs are hitherto poorly understood. Several studies on the Menderes Massif led to different interpretations of structural controls on the location of hot springs and of the heat source origin. This paper describes geological evidence showing how heat is transmitted from the abnormally hot mantle to the geothermal reservoirs. On the basis of field studies, we suggest that crustal-scale low-angle normal faults convey hot fluids to the surface and represent the first-order control on geothermal systems. At the basin scale, connected on low-angle normal faults, kilometric high-angle transfer faults are characterized by dilational jogs, where fluids may be strongly focused. In addition, favourable lithologies in the basement (e.g., karstic marble) could play a critical role in the localization of geothermal reservoirs. Finally, a compilation of geochemical data at the scale of the Menderes Massif suggests an important role of the large mantle thermal anomaly, which is related to the Hellenic subduction. Heat from shallow asthenospheric mantle is suggested to be conveyed toward the surface by fluid circulation through the low-angle faults. Hence, geothermal activity in the Menderes Massif is not of magmatic origin but rather associated with active extensional tectonics related to the Aegean slab dynamics (i.e., slab retreat and tearing).

Keywords Menderes Massif · Structural control · Detachment · Transfer fault · Hot mantle anomaly · Slab dynamics

Electronic supplementary material The online version of this article (<https://doi.org/10.1007/s00531-018-1655-1>) contains supplementary material, which is available to authorized users.

✉ Vincent Roche
vincent.roche@cnrs-orleans.fr

¹ ISTO, UMR7327, Université d'Orléans, CNRS, BRGM, 1A rue de la Férollerie, 45071 Orléans, France

² Sorbonne Université, CNRS-INSU, Institut des Sciences de la Terre Paris, IStEP UMR 7193, 75005 Paris, France

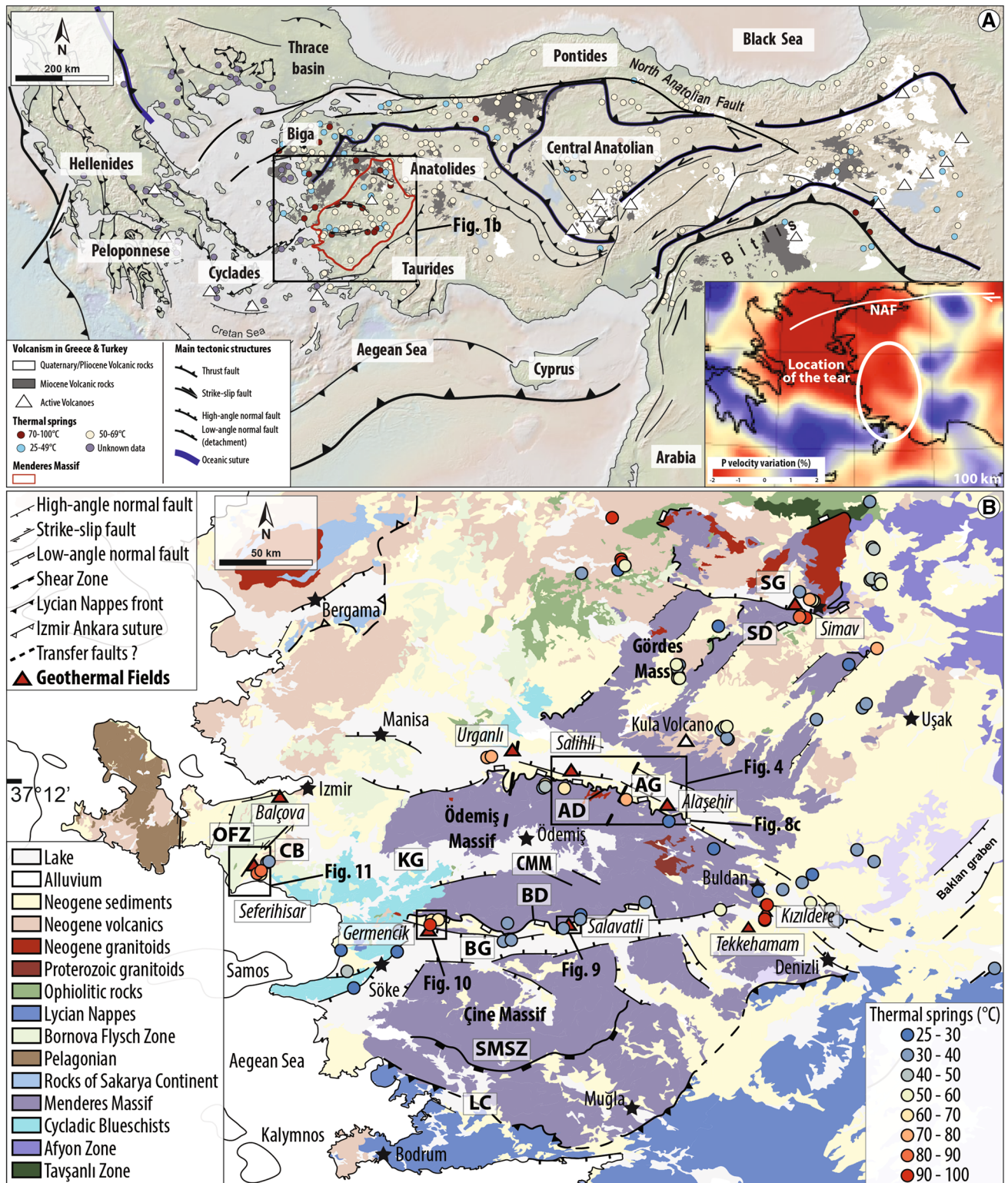
³ Middle East Technical University, Department of Geological Engineering, Üniversiteler Mahallesi, Dumlupınar Bulvarı No: 1, 06800 Ankara, Turkey

⁴ Center for Global Tectonics and State Key Laboratory of Geological Processes and Mineral Resources, China University of Geosciences, 388 Lumo Road, Hongshan District, Wuhan 430074, Hubei, China

⁵ Municipality of Salihli, Manisa, Turkey

Introduction

The high heat-flow driving active geothermal systems is often believed to find its source in portions of crust invaded by magmas, but some of significant geothermal provinces are considered amagmatic namely not of magmatic origin in terms of heat source (i.e., no magmatic intrusions in the upper crust). In this case, large-scale processes (e.g., slab dynamics) inducing large-scale thermal anomalies are favoured, as for the Basin and Range Province in the Western US. In this extensional context, geothermal systems have been described as amagmatic in origin (e.g., Benoit 1999; Blackwell et al. 2000; Faulds et al. 2004, 2011). The exact origin of heat remains debated and, for instance, magmatic underplating under the overriding plate (Wannamaker et al. 2006) and/or shear heating in the mantle in actively deforming area (e.g., Roche et al. 2018) are some hypothesis of heat source possibilities.



Despite the well-documented existence of large-scale seismic velocity anomalies in the mantle of the Eastern Mediterranean region (e.g., De Boorder et al. 1998), very few studies have actually considered such amagmatic geothermal provinces in their large-scale geodynamic contexts

(e.g., Roche et al. 2015, 2016, 2018; Gessner et al. 2017). The path of heat transport from mantle to surface, either conductive or through advection of hot fluids, remains to be described in such environments. The Menderes Massif is one of the best examples, where such a description can

Fig. 1 Tectonic map of Eastern Mediterranean region highlighting the main tectono-metamorphic domains and showing location of the study area. Modified from Jolivet et al. (2013) and Gessner et al. (2013). **a** Simplified tectonic map showing major thermal occurrences based on a compilation of several data sources (Akkus et al. 2005; Bayram and Simsek 2005; Mendrinou et al. 2010; Andritsos et al. 2015) and spatial distribution of Upper Tertiary–Quaternary volcanic rocks (from the geological map of the MTA). Note that white triangles indicate active volcanoes. Base maps made with *GeoMapApp* (<https://www.geomapapp.org>). Tomographic model of Piro-mallo and Morelli (2003) showing the Vp anomalies at the ~100 km depth in the bottom right corner of this figure. The white circle illustrates the schematized position of the slab tearing. Note that NAF is the abbreviation for North Anatolian Fault. **b** Tectonic and geological map of the Menderes Massif modified from the geological map of the MTA and Bozkurt et al. (2011). Red triangles represent main geothermal areas of the Menderes Massif, from Faulds et al. (2010) and Kaya (2015). Thermal spring locations correspond to our study, and to the studies from Akkus et al. (2005) and Bayram and Simsek (2005). Also indicated is the position of Figs. 4, 8c, 9, 10 and 11. Main structures and grabens are indicated in abbreviations: *AD* Alaşehir detachment, *AG* Alaşehir graben, *BD* Büyük Menderes detachment, *BG* Büyük Menderes graben, *CB* Cumaovası basin, *CMM* Central Menderes Massif, *KG* Küçük Menderes graben, *LC* Lycian contact, *OFZ* Orhanlı fault zone, *SMSZ* Southern Menderes shear zone, *SD* Simav detachment, *SG* Simav graben

be done, from the mantle to the actively extending crust, up to the geothermal reservoirs.

The Menderes Massif is recognized as an active geothermal area, where extensional or transtensional tectonics is accompanied by elevated heat-flow values ($\sim 100 \text{ mW m}^{-2}$), which appear to extend to almost the entire Aegean domain (Erkan 2014, 2015). There, high heat flow estimated by Jongasma (1974) may correspond to the low P-wave seismic velocity zone described by Piro-mallo and Morelli (2003). Surprisingly, magmatic activity and related volcanism have been very sparse there in the recent period (i.e., Pliocene and Quaternary); the unique volcanic activity occurred in the Kula volcanic field during the Quaternary between 2 and 0.2 Ma (e.g., Richardson-Bunbury 1996; Bunbury et al. 2001; Maddy et al. 2017), where geothermal activity is absent. Existing models suggest probable magmatic reservoirs in the upper crust as heat source of the geothermal system in this area, more or less connected with the Kula basaltic activity (e.g., Simsek 1985; Filiz et al. 2000; Karamenderesi and Helvacı 2003; Yilmazer et al. 2010; Bülbül et al. 2011; Özen et al. 2012; Özgür and Karamenderesi 2015; Ozdemir et al. 2017; Alçiçek et al. 2018). Nonetheless, others authors have also suggested a deeper and larger heat source triggered by slab dynamics (i.e., asthenospheric mantle flow due to slab rollback and tearing; e.g., Kaya 2015; Roche et al. 2015, 2016, 2018; Gessner et al. 2017). It is then worth studying the consequences of these processes on the distribution of heat at the surface. In this case, recent tectonic activity and related graben structures have a major interest, because they could control the fluid flow processes

(e.g., Tarcan and Gemici 2003; Faulds et al. 2010; Haizlip et al. 2013; Koçyiğit 2015; Kaya 2015; Hakkıdır et al. 2015).

Consequently, this study is dedicated to a multi-scale analysis of the different identified features of several geothermal fields of the Menderes Massif. We present a detailed structural analysis of main geothermal fields (i.e., Salihli, Alaşehir, Salavatlı and Seferihisar, Kızıldere, Germencik) to better characterize the fluid flow pattern. It is critical to evaluate which type of faults and which parts of them are most favourable for focusing geothermal activity. Our results are then discussed at different scales including that of the “Menderes geothermal Province”. At the scale of lithosphere–mantle interactions, we use a broad compilation of mantle–He and oxygen–hydrogen isotopic data to propose and discuss a new conceptual model explaining the regional thermal anomaly with reference to geodynamic processes.

Geological setting

The Eastern Mediterranean region

During the Cenozoic, the Eastern Mediterranean region (Fig. 1a) has undergone a two-step tectono-metamorphic evolution. First, in the late Cretaceous–Eocene, the convergence of Africa and Eurasia has led to the closure of the Izmir-Ankara Ocean and to the accretion of subducting continental and oceanic lithospheres (Bonneau and Kienast 1982; Dercourt et al. 1986; Jolivet and Brun 2010). Second, since the Oligo-Miocene, the kinematics in Mediterranean region has been mainly controlled by the southward retreat of the African slab responsible for back-arc extension (e.g., Malinverno and Ryan 1986; Jolivet and Faccenna 2000; Jolivet and Brun 2010; Ring et al. 2010). The Oligo-Miocene geological evolution of the Aegean region, including the Menderes Massif and the Cyclades, results from this episode of slab rollback (e.g., Seyitoğlu and Scott 1991, 1996; Seyitoğlu et al. 1992; Jolivet et al. 1996). In addition, recent studies based on geochemical analyses (e.g., Dilek and Altunkaynak 2009; Ersoy et al. 2010; Prelević et al. 2012), on tomographic models (e.g., De Boorder et al. 1998; Biryol et al. 2011; Salaün et al. 2012) and on tectonic and magmatic evolution in this area (Dilek and Altunkaynak 2009; Jolivet et al. 2015; Menant et al. 2016; Govers and Fichtner 2016) invoke the particular slab dynamics beneath western Turkey, which would be characterized by a slab tear since the Miocene (Jolivet et al. 2015) (Fig. 1a). The complex geometry of subduction zones and the tight arcs characterizing the Mediterranean region as a whole are direct consequences of slab retreat and slab tearing (Wortel and Spakman 2000; Spakman and Wortel 2004; Faccenna et al. 2004, 2006; Govers and Wortel 2005). Beside the heat wave caused by the advection of hot asthenosphere to shallow depths during retreat,

slab tearing tends to efficiently localize deformation, and to facilitate high-temperature metamorphism, crustal melting, granitic intrusions and fluid circulations (Jolivet et al. 2015; Menant et al. 2016; Roche et al. 2018). Therefore, magmatic activity during the Miocene was intense in western Turkey, but it has significantly decreased since 12 Ma (e.g., Ersoy et al. 2010). In addition, this slab dynamics has a direct consequence on Moho depth, estimated only at ~25 to 30 km in the Menderes Massif [based on geophysical data such as receiver functions computed from teleseismic earthquakes from Karabulut et al. (2013); deep seismic reflection data from Çiftçi et al. (2011); Bouguer gravity data from Altinoğlu et al. (2015) and conductivity data from Bayrak et al. (2011)].

The current tectonic evolution in this region is mainly controlled by the westward motion of Anatolia (Reilinger et al. 2006) and by N–S extension, both consequences of the same slab roll-back process complicated by several episodes of slab tearing (e.g., Faccenna et al. 2006; Jolivet et al. 2013, 2015). This direction of extension is also well constrained by the orientation of regional-scale anisotropic fabrics, suggesting a large-scale viscous flow in the lower crust and lithospheric mantle since the Miocene (Endrun et al. 2011).

The Menderes Massif

The Menderes Massif is located in the back-arc domain of the Hellenic subduction zone in the western part of Turkey (Fig. 1a, b), and constitutes a part of the Anatolide–Tauride block. After a first episode of nappe stacking and crustal thickening (e.g., Collins and Robertson 1998; Ring et al. 1999; Gessner et al. 2001a), the thickened crust of the Menderes Massif has undergone an NNE–SSW post-orogenic extension stage since the Oligo–Miocene (e.g., Seyitoğlu and Scott 1991; Seyitoğlu et al. 1992; Bozkurt and Oberhänsli 2001; Bozkurt et al. 2011). Considered as a single large metamorphic core complex, this massif has recorded a controversial two-stage exhumation process. According to Ring et al. (2003), these two stages are symmetrical, first along the south-dipping Lycian and north-dipping Simav detachments on the southern and northern edges of the massif, and then located in the Central Menderes Massif (CMM) along the Alaşehir and the Büyük Menderes detachments (Fig. 1b). However, Seyitoğlu et al. (2004) challenged the first stage of exhumation suggesting that this massif was exhumed initially as an asymmetric core complex in the Early Miocene. In any case, this post-orogenic extension has led to the exhumation of three submassifs, from north to south: the Gördes, Ödemiş (corresponding to the CMM) and Çine submassifs. These submassifs are separated by E–W striking half-grabens that are seismically active. The northern part of the Gördes submassif is limited in the north by the Simav graben, the Ödemiş submassif by the Alaşehir

graben (also known as Gediz graben) to the north, and by the Büyük Menderes graben to the south (Fig. 1b, see more details in the Appendix for the studied grabens).

Post-orogenic extension was thus accommodated by three main detachment faults (i.e., low-angle normal faults) in the central and northern submassifs, namely:

1. the Büyük Menderes detachment along the northern margin of the Büyük Menderes graben with top-to-the-S kinematic criteria (Fig. 1b, e.g., Emre and Sözbilir 1997; Gessner et al. 2001b; Ring et al. 2003);
2. the Alaşehir detachment (also named Gediz detachment, Lips et al. 2001) along the southern margin of the Alaşehir graben with top-to-the-N sense of shear (Fig. 1b, e.g., Emre 1992; Hetzel et al. 1995a, 2013, b; Gessner et al. 2001b; Sözbilir 2001; Seyitoğlu et al. 2002; Işık et al. 2003; Bozkurt and Sözbilir 2004) and
3. the Simav detachment, later cut by the high-angle Simav normal fault that bounds to the south the Simav graben with top-to-the-NE kinematic indicators (Fig. 1b, e.g., Seyitoğlu 1997; Isik et al. 1997, 2004; Işık and Tekeli 2001).

However, the exhumation history of the Menderes Core complex and the multi-staged activity of the detachments remain matters of debate. Several authors suggest that the Alaşehir graben formation is controlled by (1) low-angle normal faults that have been active since the inception of the basin, and then by (2) more recent high-angle faults cross-cutting the earlier ones (e.g., Hetzel et al. 1995a, b; Emre and Sözbilir 1997; Sözbilir 2001; Oner and Dilek 2011). For others, the initiation of the graben involved high-angle normal faults that gradually became low angle with time (e.g., Gessner et al. 2001b; Bozkurt 2001; Seyitoğlu et al. 2002; Purvis and Robertson 2005; Çiftçi and Bozkurt 2009, 2010; Demircioğlu et al. 2010; Seyitoğlu et al. 2014). According to Seyitoğlu and Işık (2015), this last hypothesis may explain the large range values of ages from the Alaşehir detachment, explaining a continuum of deformation since Early Miocene in the framework of a rolling hinge model (Buck 1988) for the formation of the grabens and exhumation of the CMM (e.g., Gessner et al. 2001b; Seyitoğlu et al. 2002, 2014). Note that syn-extensional Miocene granitoid intrusions are also recorded in the footwall of the Alaşehir and Simav detachments (e.g., Hetzel et al. 1995b; Isik et al. 2003, 2004).

The early Miocene evolution of the Menderes Massif is dominated by high-angle E–W striking normal faults that root into (Seyitoğlu et al. 2002) or cut the current low-angle normal faults (e.g., Koçyigit et al. 1999; Yilmaz et al. 2000), and control basin sedimentation (i.e., the initiation of the Alaşehir and Büyük Menderes grabens formation; e.g., Seyitoğlu 1997; Seyitoğlu et al. 2002). During Pliocene–Quaternary times, another set of high-angle normal

faults is recorded, controlling the youngest grabens such as the Küçük Menderes and Simav grabens (Seyitoğlu et al. 2014) and the current geometry of the basin (Bozkurt and Sözbilir 2004; Kent et al. 2016). Furthermore, an additional distributed strike-slip tectonics with a normal component is well observed in the Alaşehir graben with high-angle N–S striking faults crosscutting the Neogene sediments (e.g., Çiftçi and Bozkurt 2010; Yilmazer et al. 2010; Oner and Dilek 2011) and affecting the basement of the Menderes Massif (see black dotted line in the Alaşehir graben in Fig. 1b). Similar strike-slip faults are observed in the Büyük Menderes graben, which can be interpreted as transfer faults (e.g., Çifçi et al. 2011).

Geothermal setting in the Menderes Massif

Thermal anomalies at different scales

At first glance, there is a strong correlation between the distribution of geothermal fields with its hot springs and the location of detachments (Fig. 1b). According to recent studies (e.g., Roche et al. 2015, 2016, 2018; Kaya 2015; Gessner et al. 2017), these large-scale structures may represent the first-order control on geothermal fields in this massif. In that instance, Gessner et al. (2017) showed that most of hotter thermal springs are located in areas of structural complexity such as Seferihisar, Denizli, Salihli and Alaşehir. Similar correlations between high heat-flow values and complex graben structures are emphasized by many studies (Tezcan 1995; Pfister et al. 1998; Erkan 2014, 2015). For instance, Erkan (2014) estimated heat-flow values of 85–90 mW m⁻², locally higher than 100 mW m⁻² in the northeastern part of the Alaşehir graben. These data are in accordance with locations of several geothermal reservoirs of interest, but also with shallow Curie-point depth (CPD) published in the Menderes Massif area (Aydın et al. 2005; Dolmaz et al. 2005; Bilim et al. 2016). According to Bilim et al. (2016), the average of CPD in the whole Menderes area (assumed to represent the depth of the 580 °C isotherm, Schlinger 1985; Ross et al. 2006) is ca. 9.5 km with a shallowest point at 6.21 km around the Kula basaltic area. A thermal anomaly thus encompasses the whole Menderes Massif. The same authors also suggest that locations of geothermal fields belonging to the Büyük Menderes graben area coincide with the lowest values of the magnetic intensity, which are aligned along the boundary fault of this graben. Furthermore, using the magnetotelluric method through the northern part of the Menderes Massif, Ulugergerli et al. (2007) proposed a large partial melting zone located at ~12 km depth and deep intrusions (i.e., ~15 km depth) located below the Simav graben and the Kula volcano, therefore, suggesting abnormal high-temperature values.

To sum-up, all these studies confirm that thermal anomalies in the Menderes Massif are observed with different wavelengths (i.e., crustal scale to geothermal field scale), thus different depths. The short wavelength anomalies result from shallow depth processes and those with long wavelength (crustal scale) from deep processes, and thus large-scale dynamics (e.g., Roche et al. 2015, 2016, 2018; Gessner et al. 2017). However, the plumbing system (i.e., circulation pathways) of such hot crustal fluids is not yet properly understood.

Synthesis of fluids and isotopes

Studies on oxygen and hydrogen isotopes of the main geothermal fluids

Many studies on the isotopic composition of water samples in the CMM area have been performed (Fig. 2; Filiz et al. 2000; Özgür 2002; Tarcan and Gemici 2003; Özen et al. 2012; Baba et al. 2014). To the first order, they show that most of the data from the Alaşehir and the Büyük Menderes grabens are close to the global meteoric water line (GMWL) thus indicating a meteoric origin for most of the geothermal fluids (Fig. 2b, c). Indeed, the distribution of isotopic compositions of the thermal waters in Salihli, Aydın-Germencik, Salavatlı and Denizli-Kızıldere geothermal fields shows a meteoric origin. However, some variations in isotopic distributions can be noted. There is a clear $\delta^{18}\text{O}$ shift from the MMWL (Mediterranean Meteoric Water Line) and cold-water values (empty symbols in Fig. 2b) that indicate strong water–rock interaction for all geothermal fields (Fig. 2b, c). For example, the isotopic distribution of hot waters in Kurşunlu and in greenhouses well is located below the GMWL, which suggests a probable mixing of deep and shallow thermal waters (Özen et al. 2012). Bülbul et al. (2011) reported a similar observation from the Alaşehir geothermal field, suggesting that thermal water reservoirs are fed by ground waters of dominant meteoric origin. They estimated cold-water contributions to thermal waters ranging from 75 to 95%. Moreover, the Seferihisar geothermal field, in the Cumaovası basin, shows additional variations in isotopic compositions (Fig. 2d): isotopic values approach the isotopic value of Aegean sea water, implying a mixing with seawater related to the proximity of the Mediterranean Sea (Tarcan and Gemici 2003). Similar signatures are observed in the Söke geothermal field (Simsek 2003), with slight deviations from the MMWL line of isotopic distribution, implying an evaporation effect on cold waters (Fig. 2d). The isotopic composition of thermal waters indicates that they are of meteoric origin and then mixed with seawater in the western part of Söke, particularly near the coast.

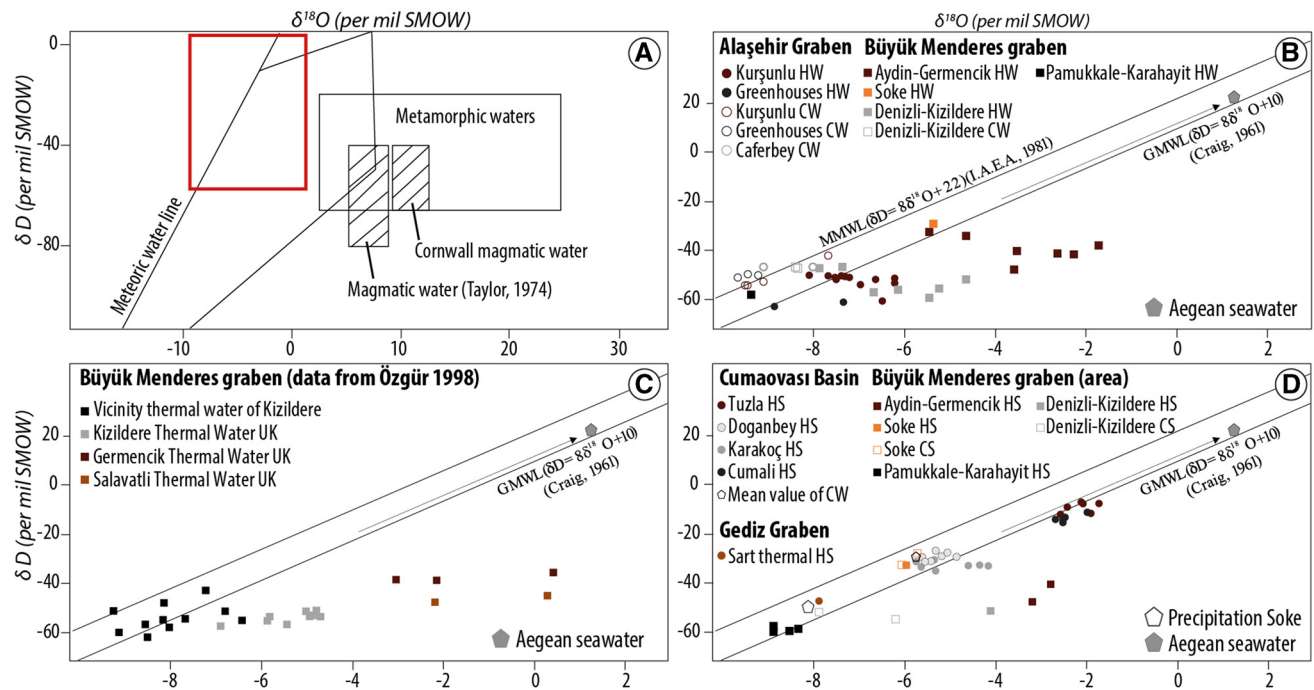


Fig. 2 δD vs $\delta^{18}O$ diagrams. **a** Plot of δD vs $\delta^{18}O$ diagram for different water types. The field of magmatic water and formation waters are taken from Taylor (1974). The field for magmatic waters from the granites of Cornwall is from Sheppard (1977). The meteoric water line is from Epstein et al. (1965). The metamorphic water field combines the values of Taylor (1974) and Sheppard (1981). Red rectangle indicates the field of all isotopic data from the Menderes Massif. **b** Stable isotope compositions of the geothermal reservoir fluids in the

studied areas showing hot and cold waters wells. *HW* hot water well, *CW* cold water well. **c** Stable isotopes of different geothermal fields in the Büyük Menderes Graben. *UK* unknown sampling locations. **d** Stable isotopes of springs in three main basins. *HS* hot spring, *CS* cold spring. Compilation of data from Filiz et al. (2000), Özgür (2002), Tarcan and Gemici (2003), Simsek (2003) and Özen et al. (2012)

Helium isotopic signature

In a tectonically active continental setting, the presence or the absence of mantle helium (^3He) in hydrothermal fluids can constrain the relationships between tectonics, magmatism and fluid circulation in faulted settings (O'niions and Oxburgh 1988; Marty et al. 1992; Kennedy et al. 1997; Kulongoski et al. 2005; Pik and Marty 2009). It has been established that the $^3\text{He}/^4\text{He}$ ratio can be used as tracer of the competing influence of crustal vs mantle volatiles in various tectonic settings (Mutlu et al. 2008). Based on the analyses of water and gas samples, and/or fluid inclusion trapped in calcite, many studies have discussed the isotopic composition of He in the Eastern Mediterranean region (Güleç 1988; Güleç et al. 2002; Shimizu et al. 2005; Güleç and Hilton 2006; Mutlu et al. 2008; Pik and Marty 2009; Karakuş 2015). Below, we present a new compilation of recent isotopic studies using the classification of Pik and Marty (2009) (Fig. 3).

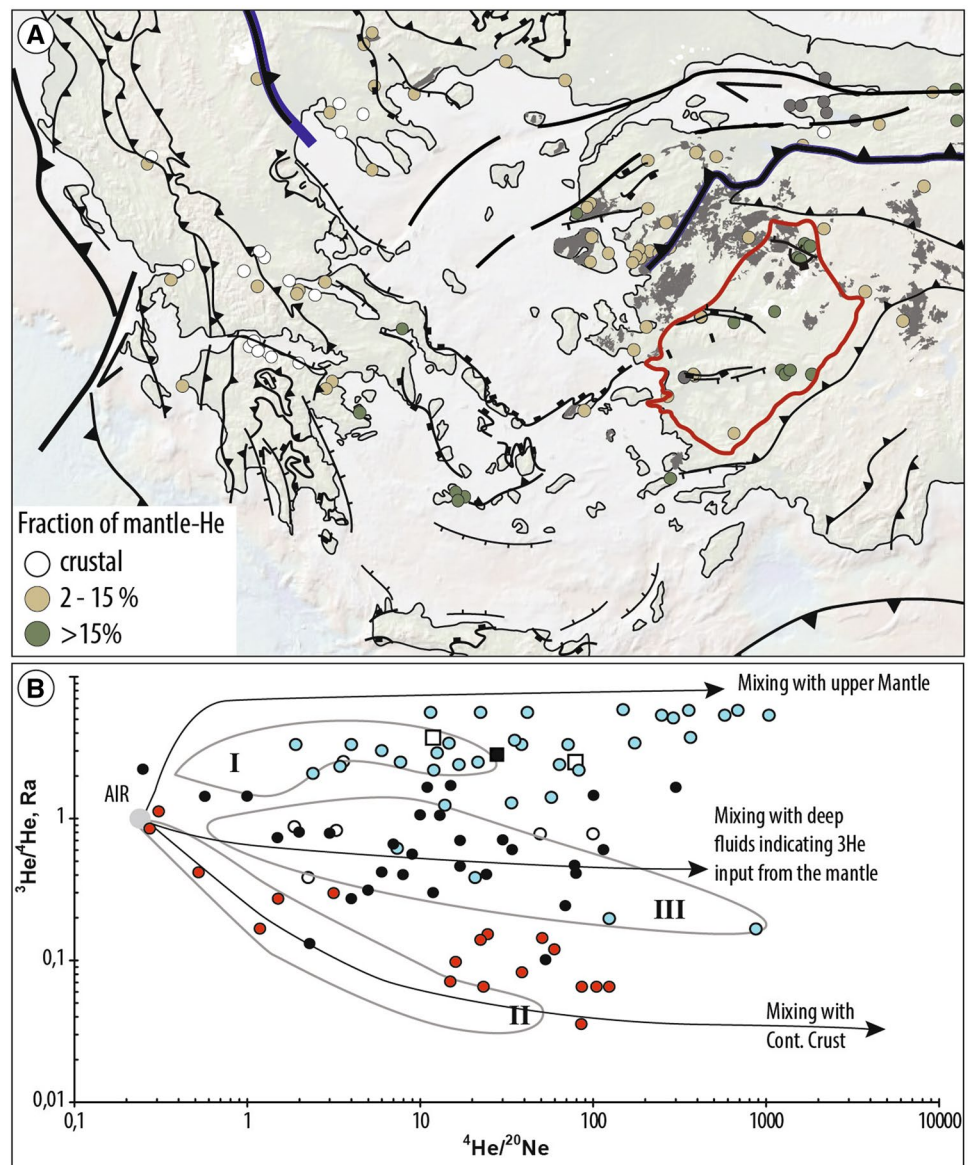
In the Aegean domain, the Corinth rift shows a crustal signature, while the Hellenic volcanic arc is characterized by high values of $^3\text{He}/^4\text{He}$ ratio, *Ra* (> 15% of mantle–He) suggesting a mantle origin (Fig. 3a). In addition, estimated

$^3\text{He}/^4\text{He}$ ratios of samples normalized to the atmospheric $^3\text{He}/^4\text{He}$ ratio range from 0.10 to 1.44 in the western part of Anatolia (Fig. 3a, b). These values are significantly higher than the crustal production value of 0.05 (Mutlu et al. 2008). Karakuş (2015) added new data on the $^3\text{He}/^4\text{He}$ ratios for the Simav geothermal field (values range from 1.36 to 1.57). The highest values of helium ratio correspond to the Quaternary alkaline activity of Kula volcano and to the Pliocene Denizli volcanics (2.52) along the Alaşehir and the eastern segment of the Büyük Menderes grabens (Fig. 3b). These results reveal a mixed origin for helium between mantle and continental crust components.

Analysis of the tectonic and structural settings of geothermal fields in the Menderes Massif at local and regional scale

In this chapter, we summarize the structural framework of several geothermal fields, to identify the main conduits for geothermal fluid flow and related reservoirs. Our field survey consisted of (1) field mapping to complement the

Fig. 3 Isotopic composition of Helium. **a** Fraction of mantle–He in hydrothermal fluids from the Aegean Anatolian domains computed from helium isotopic data, assuming mixing between a crustal component (0.04 Ra) and a mantle component (8 Ra), modified from Pik and Marty (2009). Helium isotopic data are from Pik and Marty (2009) and Karakuş (2015). **b** R/Ra diagram for the Eastern Mediterranean region from Güleç (1988), Güleç et al. (2002), Güleç and Hilton (2006), Mutlu et al. (2008), Pik and Marty (2009) and Karakuş (2015). Black dots showing data of the west Anatolian domain, red dots data of the gulf of Corinth, Blue dots data of the magmatic arc and white dots data of the back-arc region in Greece. In addition, white and black squares indicate, respectively, the Denizli and Kula areas which are located in the Menderes Massif. The fields of the three groups of hydrothermal fluids (Pik and Marty 2009), are also presented: I = arc magmatic fluids (> 15% mantle–He), II = crustal signature (< 1% mantle–He), III = other intermediate fluids (2–15% mantle–He)



existing geological and geothermal maps and (2) structural data acquisition and (3) general cross sections. We have first focus on the Alaşehir graben (Fig. 1b), where numerous geothermal wells have been drilled by MTA (General Directorate of Mineral Research and Exploration of Turkey) or by private companies since the 1980s, and where two most important geothermal fields are recognized (Salihli and Alaşehir, Fig. 4a). We will then focus on the Germencik and Salavatlı geothermal fields located along the northern margin of the Büyük Menderes half-graben (Fig. 1b). Finally, the structural framework of the Seferihisar geothermal field is also provided (Fig. 1b). A brief description of all these geothermal systems is presented in the Appendix. They are generally characterized by medium-to-high enthalpy, with reservoir temperature values ranging from 120 to 287 °C (e.g., Karamanderesi 2013; Baba et al. 2015).

Structural features of the Salihli geothermal field

At regional scale, the Alaşehir detachment is one of the best-preserved crustal structure in the study area (Fig. 5a). Both metamorphic rocks and Miocene intrusions in the footwall of the detachment present a pervasive network of kilometeric to millimetric structures developed from the ductile–brittle transition to the brittle deformation field during extension and exhumation (Fig. 4b) (e.g., Emre 1992; Hetzel et al. 1995a, b; Işık et al. 2003). Close to the main contact between the Menderes basement rocks and Neogene sediments, the foliation of basement rocks strikes E–W with low to moderate dip values toward the north and carries an N–S trending stretching lineation (Fig. 4). Most ductile kinematic indicators are top-to-the-NNE. All lithologies are deformed by asymmetric structures and folds at various

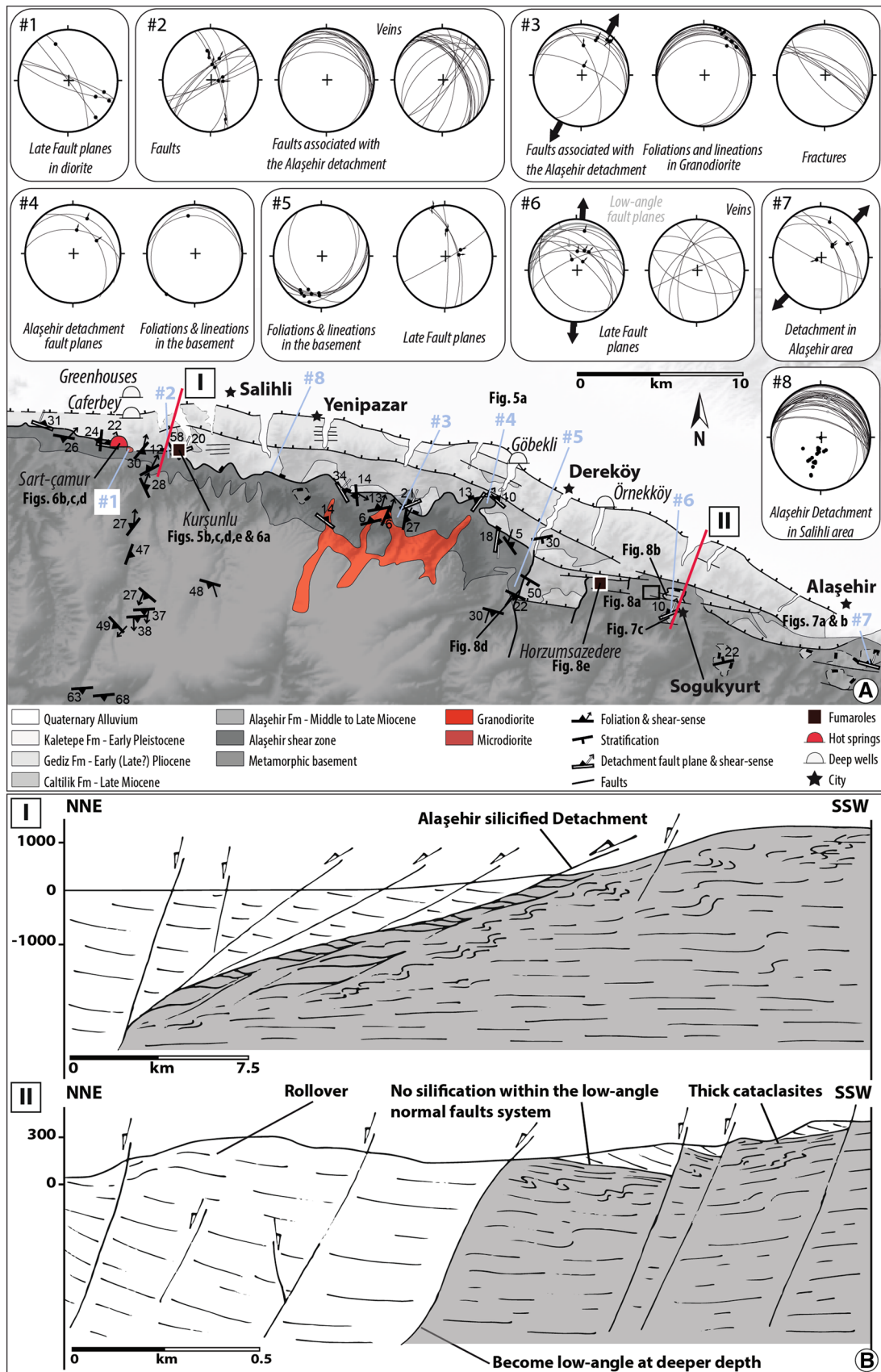


Fig. 4 Geological and tectonic map of the Alaşehir graben modified from Asti (2016). **a** Map showing main structures: the Alaşehir low-angle normal fault, E–W striking high-angle normal faults and N–S striking high strike-slip faults which are described by Çiftçi and Bozkurt (2010). Thermal springs and fumarole activity are also located in the map. Brittle structures, foliation, veins and fractures are presented in Schmidt’s lower hemisphere equal-area projection. Detailed results of the fault-slip data inversion are also presented using the Win-Tensor software (Delvaux and Sperner 2003). Also indicated is the position of Fig. 5, 6, 7 and 8. **b** Cross sections through the northern part of the Ödemiş Massif. Sections are all roughly parallel to the tectonic transport. To draw the shape of stratification, we used the bedding data of the Neogene sediments from Asti (2016). Colours show different rock types. Cross sections are indicated by red solid lines in Fig. 4a

scales consistent with top-to-the-NNE shear sense such as asymmetric boudinaged quartz veins within tight overturned folds indicating a top-to-the-NE sense of shear (Fig. 5b). On the other hand, ductile–brittle fault system corresponds to listric and gently dipping centimetric to decametric faults within schist and marble layers that may reactivate and (or) cross-cut low-angle ductile shear zones (Fig. 5c). This brittle stage is associated with slickenlines and kinematic indicators indicating also top-to-the-NNE motion (Fig. 4a, #2). Finally, the brittle detachment fault plane is well observed in the landscape (Fig. 5a), controlling the present-day topography of the CMM at regional scale and strikes E–W with a moderate dip toward the north (Fig. 4a, #8). It is associated with a thick (approximately 50 cm to 3 m) zone of cataclasites or a thick quartz-breccia vein (Fig. 5d), which locally hosts Sb–Hg(–Au) ore deposits (Larson and Erler 1993). Fault plane and associated striae (e.g., Fig. 4a, #3 and #4) are consistent with an NNE–SSW extension. In addition, vein networks mostly filled by calcite or quartz in the footwall of the detachment (Fig. 5e) present an approximately NW–SE (i.e., parallel to the detachment) and NE–SW preferred orientations (i.e., perpendicular to the detachment) (Fig. 4a, #2). This shows evidence of a significant older fluid circulation in the fault plane during the exhumation of the deeper parts of the Menderes Massif.

In the entire studied area, faults that are particularly abundant play a major role in the formation and development of longitudinal and transverse valleys (e.g., Kurşunlu valley, Alaşehir graben). Three types of plurimetric to kilometric faults, particularly frequent in this area, are observed in the field (Fig. 4a). The first one is characterized by NNE-dipping normal faults (i.e., E–W trending) and the second one is defined by sub-vertical N–S striking strike-slip faults (Fig. 4a, #2; 6a and 6b). In the second case, slickenlines are gently plunging consistently 15–30°N (Fig. 6a, c) and kinematic indicators indicate a main dextral movement with a slight normal component. Locally, these faults are accompanied with a cluster of calcite veins as dilational jog structures (Fig. 6d). The third type of faults consists in a set

of conjugate faults strikes NE–SW and dips with an approximately 60° mean dip angle, is well developed in quartzite levels in the Kurşunlu valley (Fig. 4a, #2). The different fault sets, including the detachment and the associated high-angle E–W conjugate normal faults and the N–S strike-slip faults to NE–SW faults, are compatible with N–S extension, where strike-slip faults act as transfer zones between extensional blocks. All these faults affect the basement and the Neogene sediments, but the chronologic relationships are not clear in the field.

Structural features of the Alaşehir geothermal field

The Alaşehir geothermal field is located between Alaşehir and Salihli in the eastern part of Alaşehir graben. It is one of the most important geothermal areas characterized by the highest reservoir temperature (287 °C) ever reached in Turkey (in a deep well, 2750 m, from Baba et al. (2015), Table 1). As for the Salihli geothermal field, the recent tectonic activity is assumed to control the location of the thermal springs and related geothermal reservoirs (Bülbül et al. 2011). In this area, the detachment fault plane is attested by the development of a thick zone (~ 1 m) of cataclasites (Fig. 7a). It consists of yellow and red foliated cataclasites directly overlain by unaltered Neogene sediments (Fig. 7b). Close to the kinematics recorded in the area of Salihli, striae are compatible with an NE–SW extension (Figs. 7a and 4, #7). Additional low-angle normal faults in the hanging wall of the detachment are observed between 1 m-thick cataclasites and sediments (Fig. 7c–e). Locally pseudotachylytes are observed (Fig. 7f) and medium-angle normal faults in sediments merge with the main fault plane (Fig. 7g). According to Hetzel et al. (2013), this brittle deformation stage observed in the Alaşehir detachment system was active from ~9 Ma to 4–3 Ma. This may be consistent with rapid Pliocene cooling inferred from published thermochronological data (Gessner et al. 2001b; Ring et al. 2003). While the Alaşehir detachment is well defined in the landscape at Salihli, it is, however, often crosscut by a set of E–W high-angle north-dipping normal faults in the Alaşehir area (Figs. 4b, 8a). Brittle structures, shallow- and steeply-dipping faults present a marked consistency of the extension direction (Fig. 4a, #6). Locally, fluid circulation occurs along fault planes (Fig. 8b), suggesting that these faults may also control meteoric fluid circulations. The absence of any hot springs close to the E–W striking faults suggests that these faults play as recharge pathway for reservoirs at depth.

Furthermore, another set of faults is observed at some places. At landscape scale, in the south-east of Alaşehir, we identified triangular facets within synrift sediments due to NW–SE trending high-angle normal fault (Fig. 8c). The latter are horizontally offset from 2 km toward the south in the Narlıdere area, defining an NE–SW transfer fault (Figs. 8c,

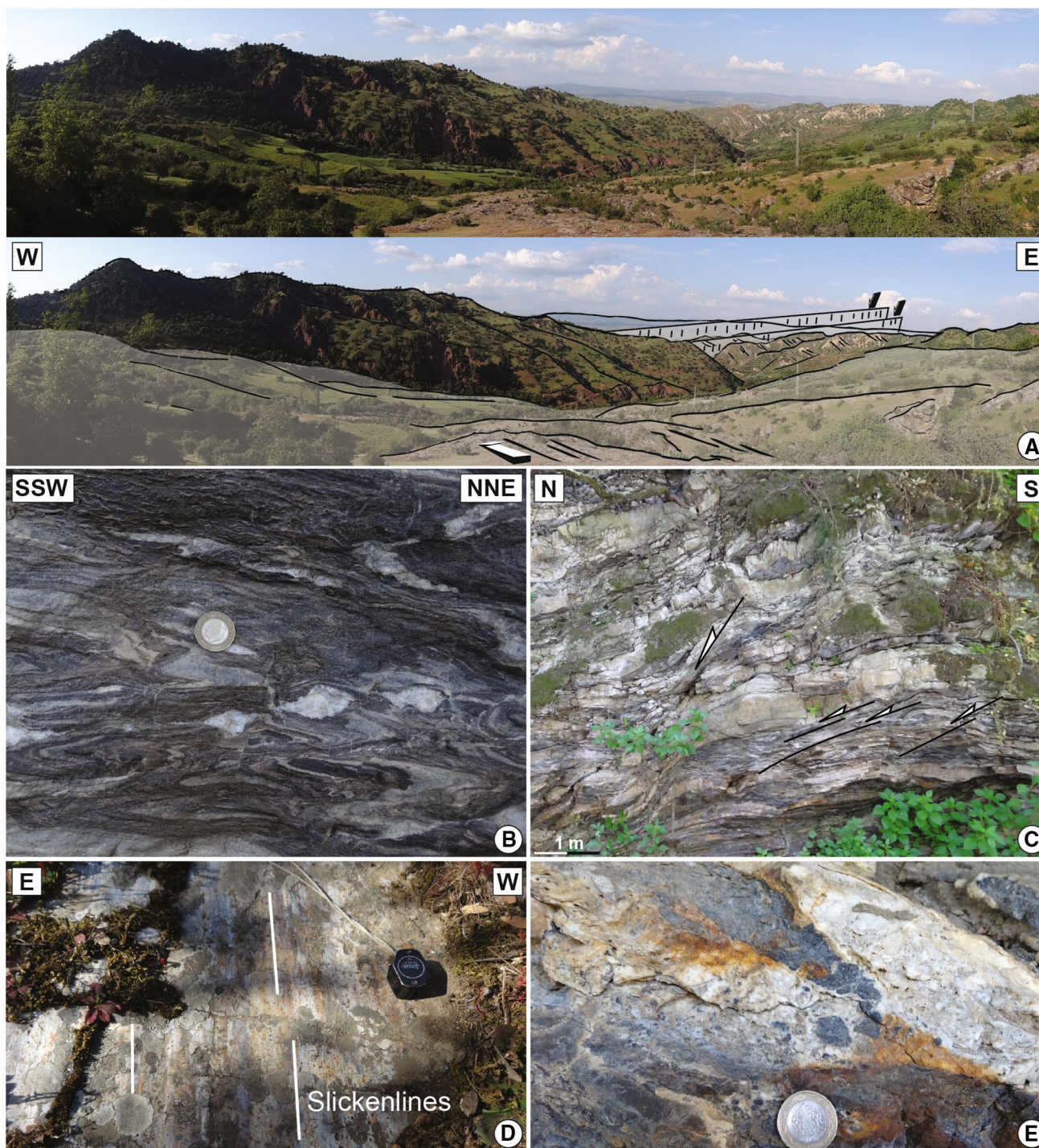


Fig. 5 Kinematic of deformation associated with the Alaşehir detachment. **a** Large-scale view of the Alaşehir detachment surface close to Salihli area. **b** Asymmetric boudins compatible with top-to-the-NNE ductile deformation in marbles layers. **c** Representative outcrop recognized as demonstrative of a brittle stage subsequently developed

after the ductile one, where shear zones are locally reactivated in the brittle field. **d** Fault plane of the Alaşehir detachment with slickenlines. **e** Calcite and quartz vein parallel to the bedding, located few meters below the main fault plane. The position of the pictures is indicated in Fig. 4a

1b for the location). Similar features are also observed in the Dereköy traverse valley, close to the Horzum Turtleback structure described by Seyitoğlu et al. (2014). There, we

identified an N–S striking high-angle fault (Fig. 8d). Fault kinematics indicates an early sinistral movement followed by normal movement (Figs. 4a, #5, 8d). The synrift sediments

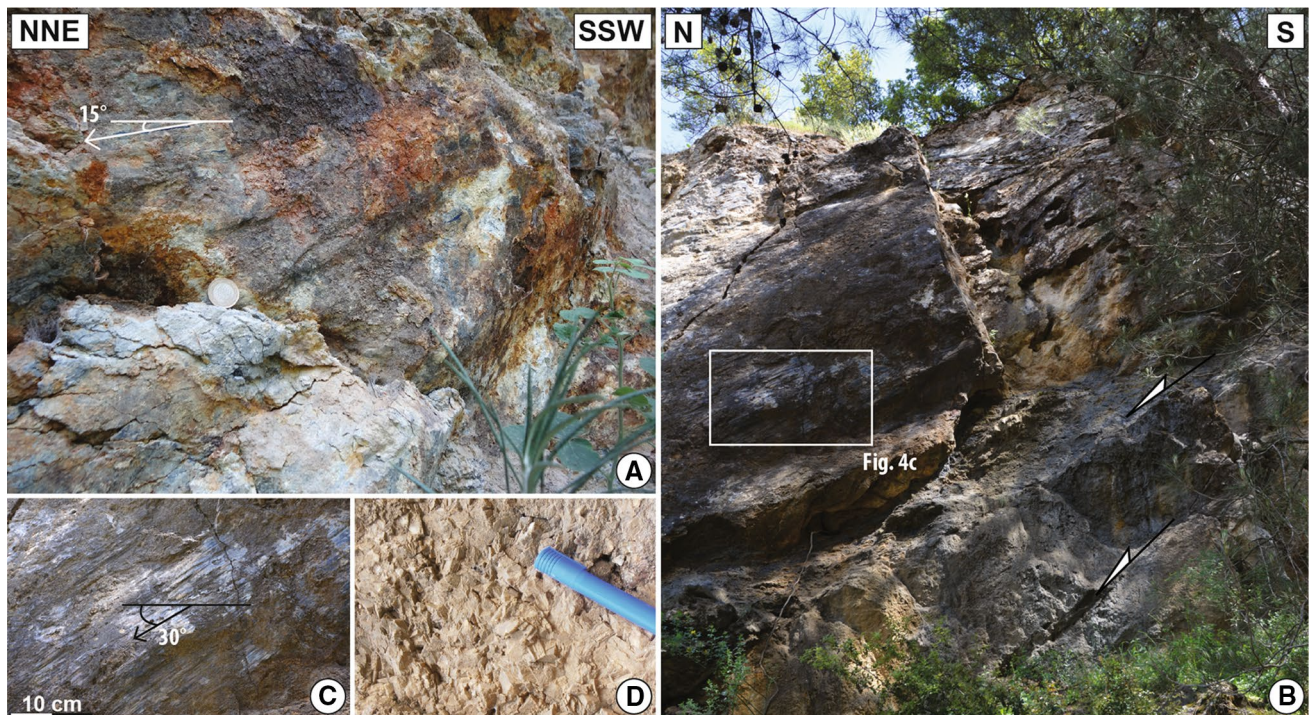


Fig. 6 Brittle deformation in the Salihli area. **a** N–S strike-slip fault in the Kurşunlu valley. **b** E–W striking normal faults are crosscut by N–S strike-slip fault. **c** Close-up view of a slip plane in the basement

of the Menderes indicating nearly horizontal with a normal component slickenlines. **d** Calcite indicating fluid circulation close to the strike-slip fault. The position of the pictures is indicated in Fig. 4a

are offset southward and face the Paleozoic basement of the detachment footwall across the valley, indicating the presence of left-lateral strike-slip fault in the vicinity of the Horzumsazdere geothermal system (black line in Fig. 4a). Close to the detachment and to these N–S strike-slip faults, a weak fumarole activity associated with a probable acidic alteration (with the typical H_2S smell) affects Neogene sediment deposits (Fig. 8e). Down in the valley, several thermal springs (medium temperatures ranging around 25 and 30 °C) reach the surface in Neogene sediments, where they form travertines.

Structural features of the Salavatlı and Germencik geothermal fields

South of the CMM, the Salavatlı and Germencik geothermal fields (Table 1 for more information) are, respectively, located on the northern flank of the Büyük Menderes graben between Sultanhisar and Köşk (Figs. 1b, 9), and at 20 km west of Aydın (Figs. 1b, 10). Similar to the previous geothermal systems, both Salavatlı and Germencik geothermal systems are located close to the Büyük Menderes detachment (Fig. 1b). Even though the age of top-to-the-north ductile deformation is still controversial (e.g., Bozkurt 2001; Gessner et al. 2001a; Seyitoğlu and Işık 2015), all studies indicate a second top-to-the-south ductile–brittle shearing event (e.g.,

Hetzel et al. 1995a, b; Gessner et al. 2001b; Bozkurt and Sözbilir 2004).

In detail, the geological sequence of the Salavatlı geothermal field is composed of Neogene sediments deposited over schist-marble sequences and augen gneiss unit (Fig. 9a). Even though the major structural feature does not clearly outcrop in this area due to strong neo-tectonic overprint, the Büyük Menderes detachment was identified in two different drill holes (Karamanderesi and Helvacı 2003). According to this study, the marble sequences in the Menderes massif at ~800 m depth host the main geothermal reservoirs. Our new field observations suggest that the general structure and the topography are mainly induced by a set of major normal- to strike-slip faults. These faults control the first-order distribution of lithologies of the two main units (augen gneiss and schist-marble sequences, Fig. 9a). The first ones are NW–SE trending faults with opposite dips (Fig. 9b, c), showing kinematic indicators of a normal movement. Here, kinematic indicators are compatible with a top-to-SW motion. The second ones are the most important and they strike N–S to NE–SW (Fig. 9c). Locally, slickenlines are well preserved and indicate a sinistral movement. These high-angle faults are characterized by a thick fault gouge and crosscut all earlier structures, such as NW–SE trending faults, and also the detachment (see the profile of Karamanderesi and Helvacı 2003). Close to these main structures, hot springs are often

Table 1 Catalogue of hot springs and geothermal fields associated with the metamorphic core complex formation in the Mendere Massif

	Geothermal fields	Depth and thickness	Flow and discharge rates	Measured temperatures	Chemical geothermometers	Lithology	Capfault and caprock
Alaşehir graben	Salihli	Reservoir depth varies from 40 to 400 m	20 L/s (K-1) and 40 to 80 L/s (other wells in Kurşunlu area)	83–94 °C	80° to 250 °C (with variability of geothermometers, e.g., SiO ₂ ; Quartz Steam Loss; Na–K–Ca)	Karstified and fractured marbles of the basement; Çaltılık Formation	Siliceous ADFP and Gediz Formation
	Alaşehir	Reservoir depth from 950 to 1500 m	30 to 35 L/s	90–92 °C			
		Reservoir depth from 1150 m and 1600 m	12 L/s (KG-1) and 6,74 L/s (Ak-2)	215 °C (A5-2)			
		Reservoir depth from 1750 to 2750 m	5–90 L/s	159–287, 5 °C			
Büyük Mendere graben	Urganlı-Turgutlu	Reservoir depth at 460 m	20 L/s	62 °C		–	–
	Germencik	Shallow reservoir depth in sediments (around 285 m)	Average flow rate 300 tph	203–217 °C	150–250 °C (Na–K and Na–K–Ca)	Miocene conglomerates and fractured rocks of the basement	Neogene clastic sediment such as clayey levels
	Salavatlı	Deeper reservoir in basement changes depending on the locality from 965 to 2432 m depth		191–276 °C			
Cumaovası basin	Salavatlı	Reservoir depth from 750 to 1923 m	Average flow rate 1480 tph	148–176 °C	160–175 °C (Giggenbach, 1986)	Fissures and fractures zones of the basement	–
	Kızılder	Reservoir depth at 3224 m	–	211 °C	–	–	–
		First reservoir depth at 400 m	Average flow rate 1400–1500 tph	148–198 °C	–	Sazak Formation (Pliocene sediments) and quartzites, marbles, gneiss of the basement	Pliocene impermeable clayey
		Second reservoir depth from 1100 m to 1200 m		200–212 °C			
	Just below the second		242 °C	250–260 °C (SiO ₂ ; Na–K–Ca)			
	Fourth reservoir depth unknown		> 250 °C	–	–	–	–
	Reservoir depth from 333 to 553 m	Total discharge rates of 130 tph	174–176 °C	–	–	Fractured mafic submarine volcanics and fractured rocks of Bornova mélange; Marbles of Mendere?	Clay-rich zones of the Neogene sediments

Table 1 (continued)

Geothermal fields	Depth and thickness	Flow and discharge rates	Measured temperatures	Chemical geothermometers	Lithology	Capfault and caprock
Simav graben	First reservoir shallow depth, 85 m Second reservoir: around 725 m	–	105 °C 162 °C	83 to 182 °C (SiO ₂) and 148 to 163 °C (Na–K–Ca–Mg)	Neogene sediments: Naşa basalt, Budğan limestone, Arnkaya and Ballıkbasi formations; Menders units?	Clayey level of Eynal, Akdağ and Sarcasu Formations

ADFP: Alaşehir detachment fault plane. Compilation data from Şimşek (1984, 2003), Simsek and Demir (1991), Yılmaz and Karamandereci (1994), Karamandereci (1997, 2013), Özgür et al. (1998a, b), Tarcan et al. (2000); Gemici and Tarcan (2002), Tarcan and Gemici (2003), Yıldırım et al. (2005), Kose (2007), Faulds et al. (2010), Kindap et al. (2010), Tekin and Akin (2011), Özen et al. (2012), Baba et al. (2014, 2015), Akin et al. (2015) and Tureyen et al. (2016)

observed (Fig. 9a), suggesting a first-order control on the emergence of thermal fluids. In addition, the presence of N–S to NE–SW trending travertine deposits in higher altitudes (Karamandereci and Helvacı 2003) confirm the key role of such structures.

The Germencik geothermal field is characterized by numerous fumaroles, hot springs, travertines and widespread hydrothermal alterations (e.g., Çamurlu and Bozköy hot springs; Fig. 10a). The Menderes basement rocks are mainly composed of Paleozoic metamorphic rocks such as the augen gneiss and schist-marble sequences, overlain by Neogene sediments. North of Çamurlu hot spring (Fig. 10a), the main foliation of metamorphic units strikes E–W and the Neogene sediments dip slightly toward the north (Fig. 10a). Locally, travertines are located close to this contact (Fig. 10a), showing that it acts as a major drain for fluid circulation. In addition, in the vicinity of Bozköy, the main foliation of metamorphic units strikes NW–SE with a low dip values (~5° to 10°) (Fig. 10b), whereas the Neogene sediments dips to the south (Fig. 10c). Such an unexpected change of dip direction may suggest a fault drag area and the possible presence of an N–S high-angle strike-slip transfer fault (Fig. 10a). Here again, the occurrence of geothermal surface expressions suggests that this type of faults favours fluid circulation (Fig. 10d). More recent tectonic features are also well expressed and consist in the development of E–W striking high-angle normal faults (Fig. 10a, f). Some of them are characterized by dip values (reaching ~60°; Fig. 10e). When such faults root in the Büyük Menderes detachment at depth (Fig. 10e), others dip steeper (~80°) and crosscut it. This latter set of faults has allowed for instance the exhumation of the Kızılcagedik Horst. This area is also characterized by numerous deep wells (see location of Ömerbeyli in Fig. 10a), and the highest temperatures were reached in the Büyük Menderes graben (~230 °C at a depth of 975 m and 1196 m; Filiz et al. 2000). Here, the E–W trending high-angle faults generate a wide fractured zone.

Structural features of the Seferihisar geothermal field

The Seferihisar geothermal field (Table 1 for more information) is located in the northern flank of the Büyük Menderes graben between Sultanhisar and Köşk (Figs. 1b, 11a). The basement of the Menderes Massif in this area is made of metamorphic rocks such as schists, marbles and local phyllite intercalations (e.g., Dora et al. 1990; Güngör and Erdoğan 2002) topped by the Bornova flysch mélange. This area is similar to the central part of the Menderes Massif, but shows some differences such as lower topography and a hidden tectonic contact localized between the Bornova flysch mélange and the Menderes Massif as suggested by Erdoğan (1990). We briefly present below the relationships between

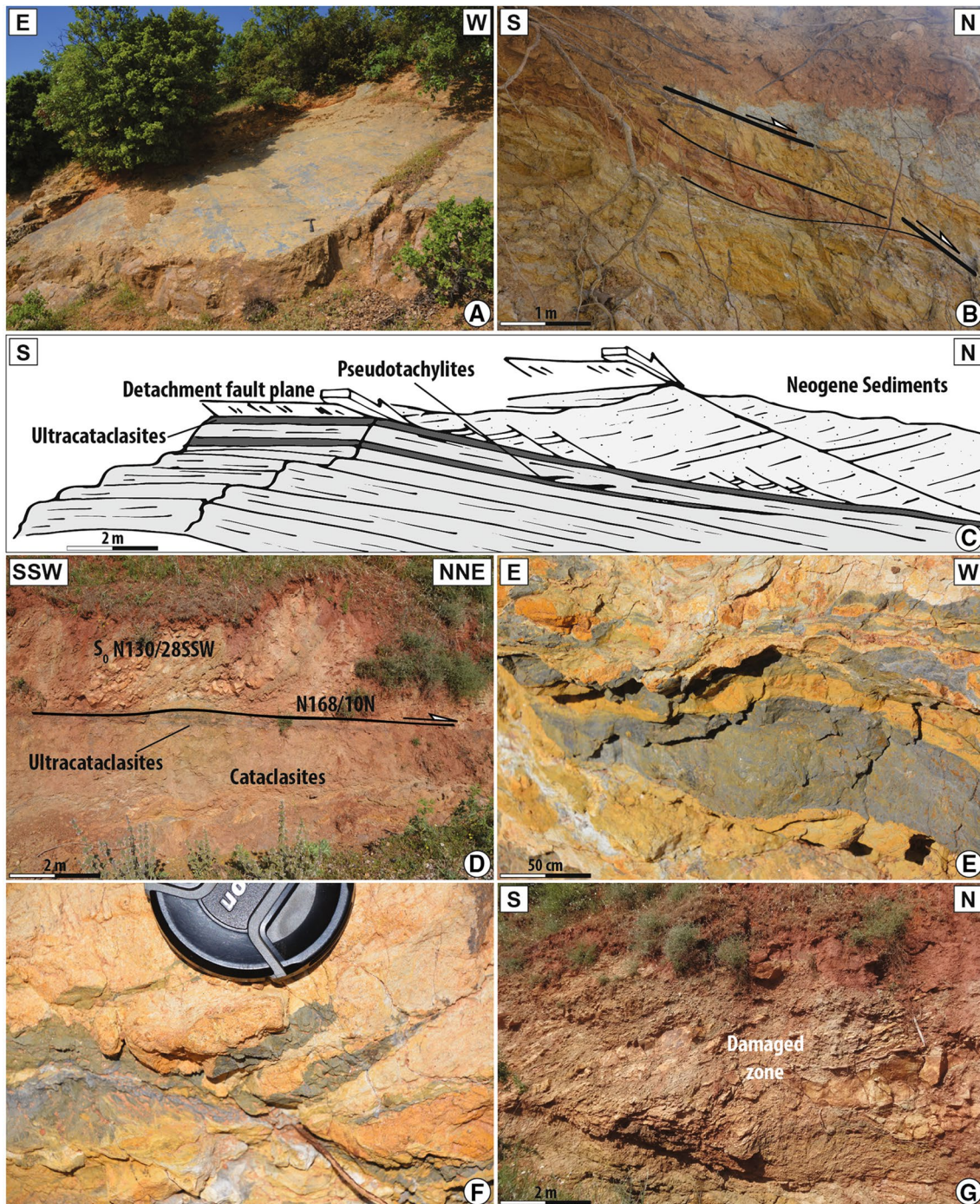


Fig. 7 Brittle deformation associated with the Alaşehir detachment in the Alaşehir area. **a** Detachment surface marked by a thick zone of cataclasites. **b** Foliated cataclasites below the main fault plane. Note that the shearing is toward the north. **c** Sketch depicting the relationships between the detachment fault plane and Neogene sediments in

the NNW of Kara Kirse. **d** Low-angle contact between metamorphic rocks (augen gneiss unit) and Neogene sediments. **e, f** Close-up view of ultracataclasites and centimetric pseudotachylites, respectively. **g** Metric damaged zone in sediments. The position of the pictures is indicated in Fig. 4a

hot spring locations and faults, and we refer the reader to the study of Ring et al. (2017) for more information about the Miocene-to-Present tectonic evolution. Field observations show that hot springs are generally located close to

NE to SW striking strike-slip faults (Fig. 11a–c). Kinematic indicators suggest a dextral strike-slip movement with lineation pitch ranging from 10°S to 22°S (Fig. 11d). In addition, these faults are characterized by multi-metric damaged

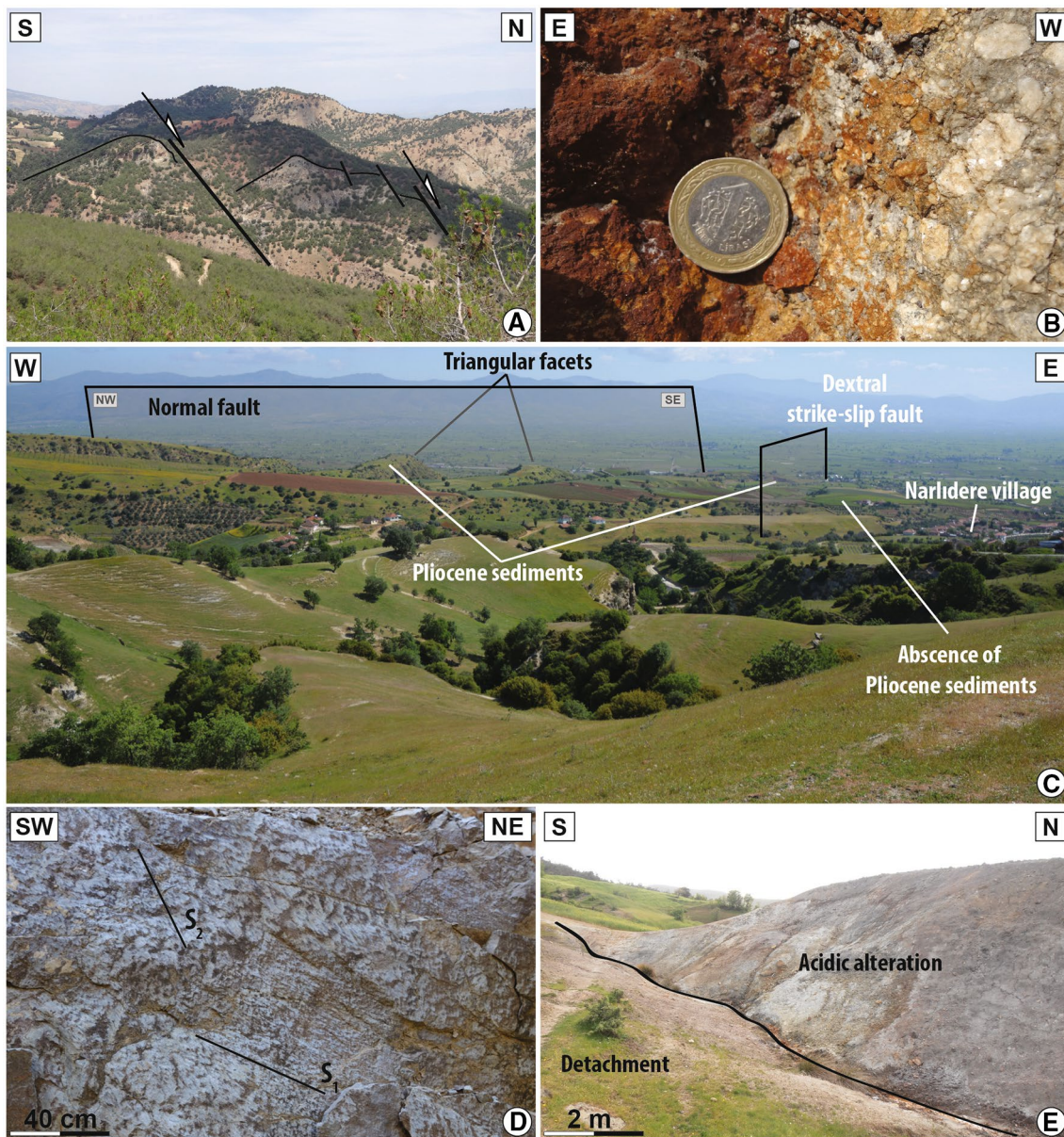


Fig. 8 Brittle deformation in the Alaşehir area. **a** Large-scale E–W high-angle normal faults. Outcrop shows hanging wall displacements toward the north. **b** Close-up view of E–W striking fault showing centimetric and angular blocs (i.e., cataclase). Note also the alteration of the basement rocks implying a probable meteoric fluid circulation during fault activity. **c** Landscape view of triangular facets in the eastern part of Alaşehir. Note the probable position of strike-slip fault.

This fault is also mapped by Oner and Dilek (2013). See location in Fig. 4a. **d** Fault plane and associated striae (two generations) of N–S striking strike-slip fault. Note that stereographic projection of striated fault planes corresponds to the number #5 in Fig. 4a. **e** Picture showing an acidic alteration related to fumarole activity. See Fig. 4a for the location of pictures

zones, locally strongly altered, attesting for recent fluid circulation. Dextral strike-slip movement is associated with dilational jogs and pull-apart structures (Fig. 11a), probably close to the intersection zones between N–S strike-slip fault and the early contact between the Bornova mélange and the Menderes basement rocks [i.e., the tectonic contact described by Erdoğan (1990)]. Furthermore, in places, E–W trending fault corridors cut these first faults (Fig. 11e). These

later sub-vertical faults show several sub-vertical and sub-horizontal slickenlines, with plunging values ranging from 85°W to 49°E and 24°E to 4°W, respectively (Fig. 11e). The calculated paleo-stress analysis suggests that kinematic indicators are compatible with an NW–SE extension (Fig. 11a). All along the main road between Cumhuriyet and Orhanlı (Fig. 11a), sandstones of Bornova mélange usually display a strong alteration. Hence, it seems reasonable to assume

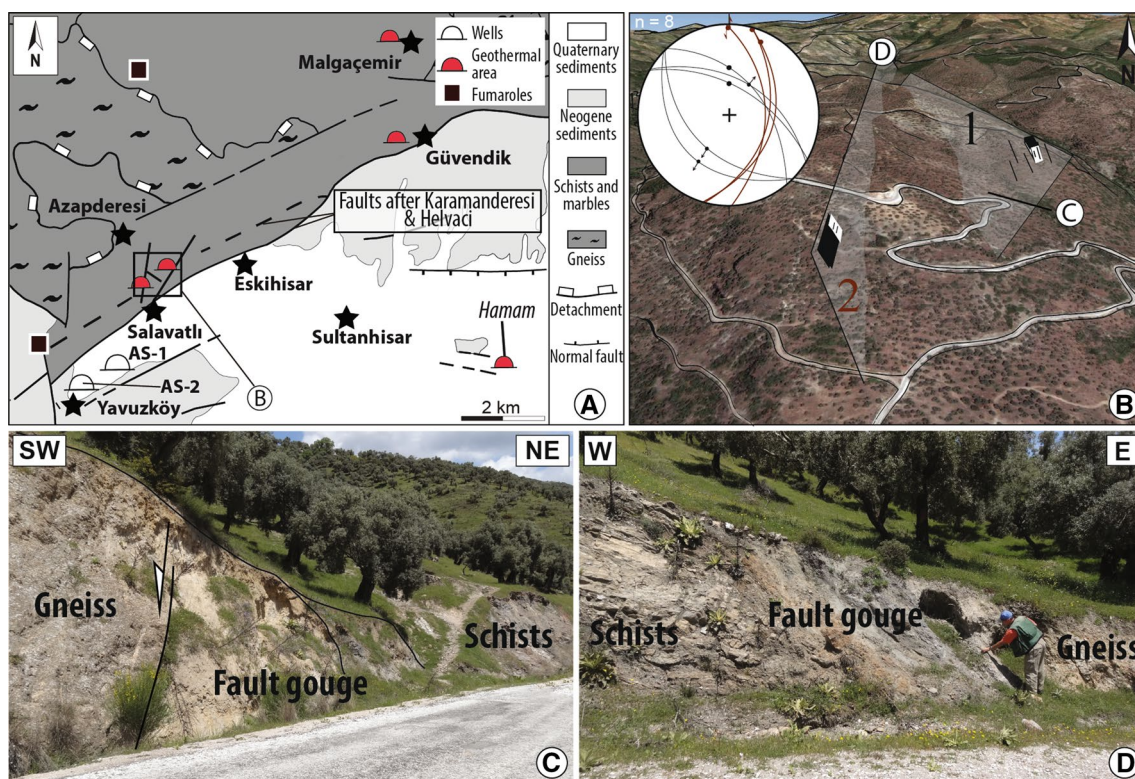


Fig. 9 Brittle deformation in the Salavatlı area. **a** Simplified geological map of Salavatlı geothermal field modified from (Karamanderesi and Helvaci 2003). **b** Google earth view of the area. Main structures and stereographic projections of faults systems are indicated. Loca-

tion is indicated in Fig. 9a. **c** NW–SE trending normal fault between gneiss and schists. **d** N–S trending faulted contact between schists/marbles sequences and gneiss. Note the metric fault breccia between these both units

the existence of others faults, which would be parallel to the previous one in this area.

Discussion

The Menderes Massif Core complex and associated geothermal fields

The genesis of a geothermal system requires source of high temperatures, reservoirs of large quantity of hot fluids (permeable structures and lithology) and its caprock. All of these features are present in the Menderes Massif, thus explaining the geothermal potential. As seen previously, thermal anomalies show different wavelengths at different depths in the Menderes Massif (i.e., crustal scale to geothermal field scale). Whereas the short wavelength anomalies result from shallow depth processes and may be associated with N–S transfer faults, the long wavelength (i.e., crustal scale or mantle scale) result from deep processes and may be associated with detachments activity. Therefore, as for many geothermal fields in western Turkey and abroad, faults appear to represent a first-order control on fluid flow and

heat transport, and thus on the location of reservoirs at depth and hot springs at the surface as leak of reservoir (Fig. 12a). In the following, we first focus on detachments at crustal scale, then we highlight the role of N–S transfer faults at basin scale.

Crustal scale: the role of detachments

At the scale of the Menderes Massif, the presence at the surface of numerous hot springs close to E–W striking, northward and/or southward dipping low-angle normal fault (Fig. 1b) suggests that detachments control fluid circulations. These latter are controlled by the current global structure of the Menderes core complex resulting from a multi-staged activity of the detachments since the Miocene. Indeed, ongoing tectonic lets the detachment systems active, and meanwhile, (1) detachment faults became incrementally split into many sections separated by transfer faults and (2) different sets of faults (i.e., E–W striking faults) merge at depth into the detachments (see Seyitoğlu et al. 2002). This complex tectonic evolution may induce an intense hydrothermal activity (e.g., silicified detachment in some areas), for instance within thick damage zone (e.g., up to 10 m of

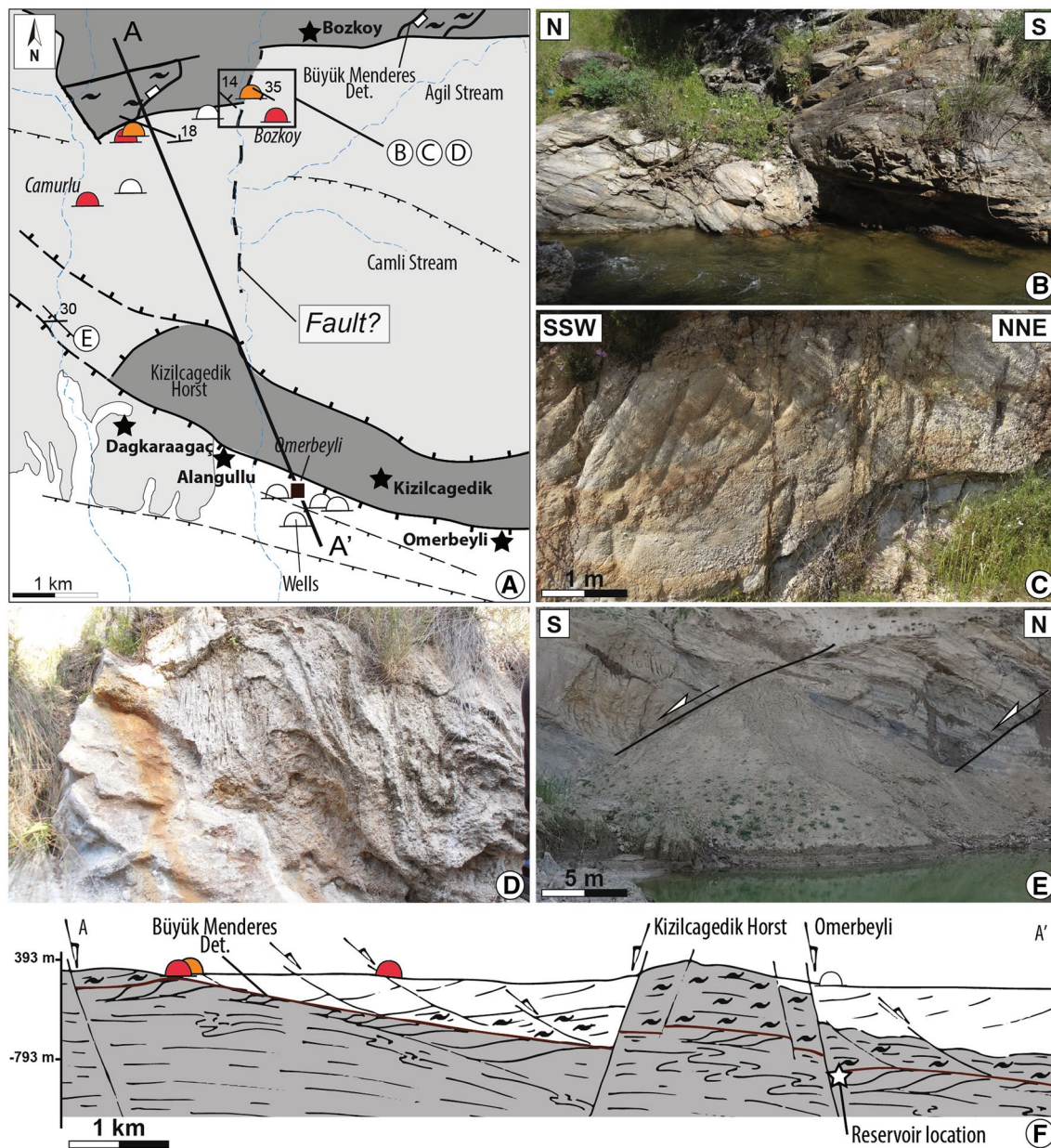


Fig. 10 Structures and geothermal activities in the Germencik geothermal field. **a** Simplified geological map of Germencik area modified from Karamanderesi (2013), showing thermal springs and fumaroles locations. **b** Shallow dipping E–W trending foliation in the basement of the Menderes units. **c** Dip inversion of the bedding in

Neogene sediments close to the basement. **d** Travertine indicating fluid circulation. **e** Sallow dipping E–W striking fault in Neogene sediments of the Büyük Menderes graben. **f** Simplified cross-section of the Germencik area (see location on Fig. 10a)

cataclasites associated with the Alaşehir detachment are present in the hanging wall and the footwall of the detachment, Fig. 7) reaching ~10 km (containing the ductile–brittle deformation associated with the detachment) according to Bozkurt (2001). One can question whether such detachment fault systems have acted as important conduits for fluid circulations since the Miocene. In any case, these structures generate zones of high fracture density and permeability that channel and host significant fluid flows in the upper crust.

They are also connected with most superficial structures (i.e., N–S transfer faults) and probably seem highly effective for heat transport and fluid circulation at deeper depth toward specific reservoirs (Fig. 12a, b).

Many studies on fluid compositions (Famin et al. 2004; Mulch et al. 2007; Gottardi et al. 2011; Hetzel et al. 2013; Quilichini et al. 2015) suggest that low-angle detachments permit pervasive meteoric fluid flow downward and/or upward along detachment fault planes, reaching depths of

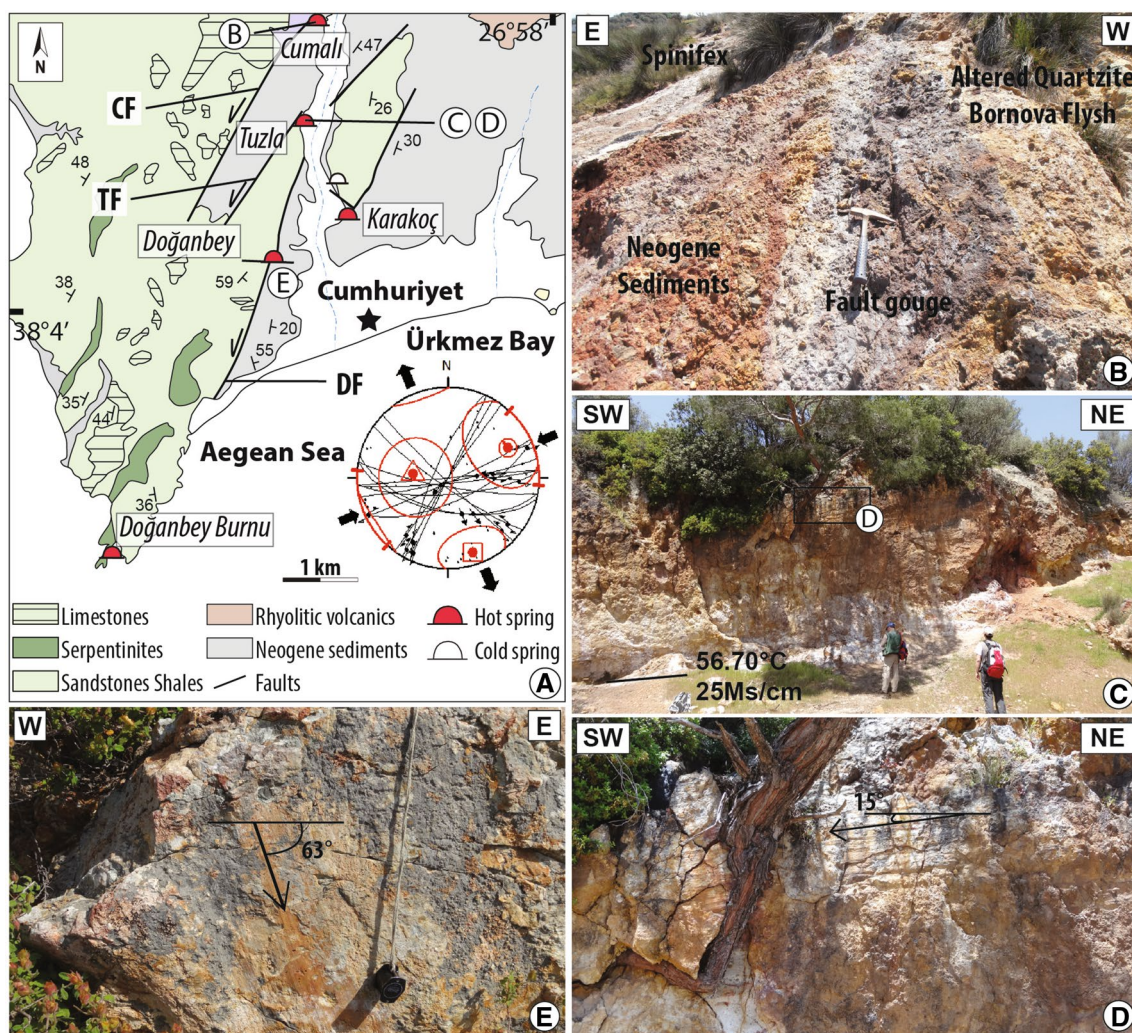


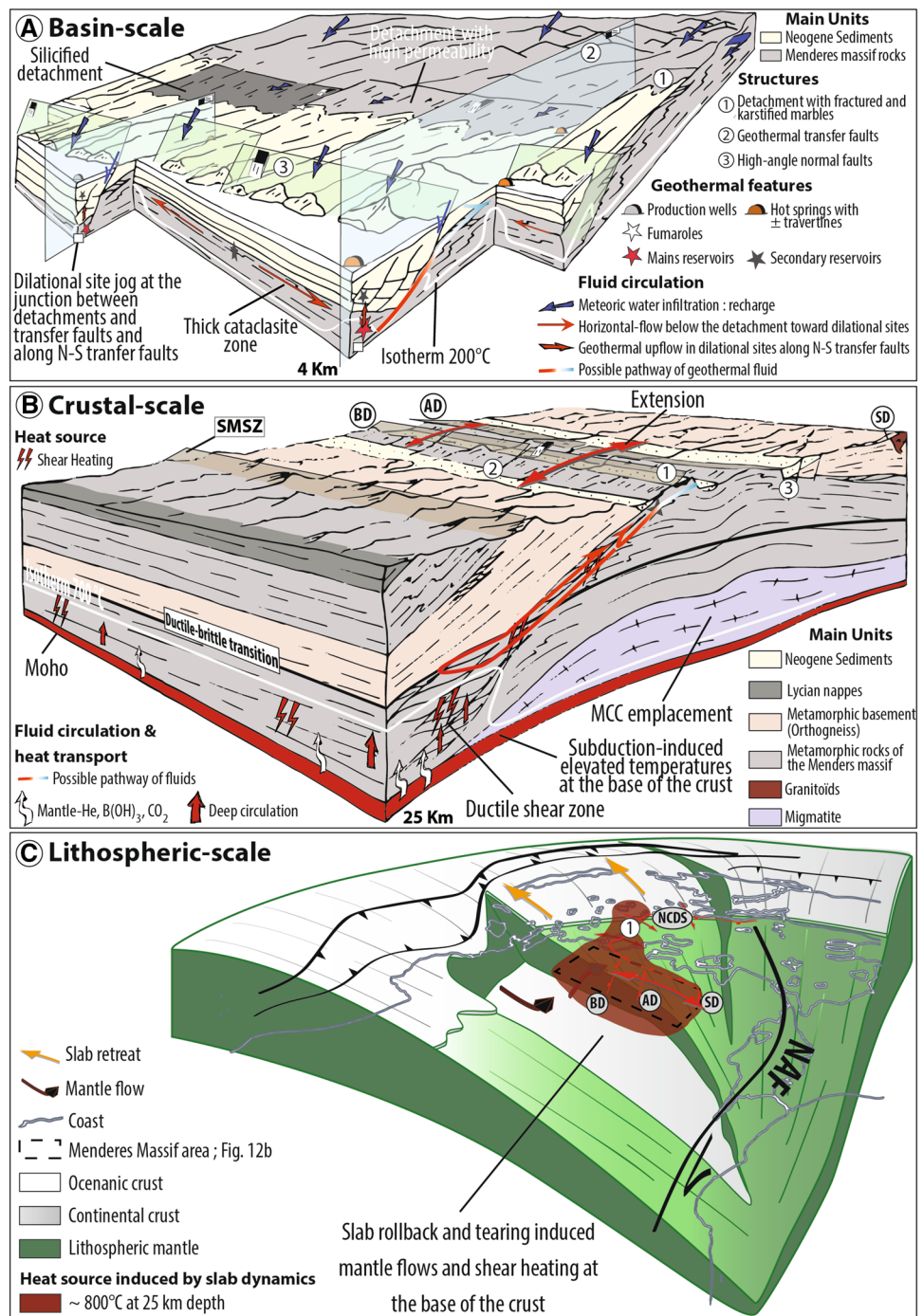
Fig. 11 Brittle deformation in the Seferihisar area. **a** Simplified tectonic and geological map of Seferihisar geothermal areas showing main structures: the Cumali Fault (CF), the Tuzla Fault (TF) and the Doğanbey Fault (DF). Modified from Genç et al. (2001) and Drahor and Berge (2006). Also are represented stereographic projections of striations and kinematics of the main fault planes. **b** CF showing the altered contact between the basement and Neogene sediments.

10–15 km. In addition, isotopic studies show the presence of small amounts of deep CO_2 , H_2S , B and He in thermal waters (see our compilation, Sect. 3.2). We thus suggest that large-scale detachment faults may represent the conduits allowing the escape of helium to the surface in the Menderes Massif. In others words, fault-controlled circulation of meteoric fluids is the dominant mechanism to explain the migration of mantle volatiles from the ductile–brittle transition zone to the near-surface (Fig. 12b) (Mutlu et al. 2008; Jolie et al. 2016). Brittle fault systems are thus probably connected at depth with ductile shear zones (Fig. 12b).

Ductile shear zones may indeed represent efficient pathways for hydrothermal fluids (e.g., Oliver 1996; Taillefer

et al. 2017). Two main mechanisms explain the fluid migration in the deeper part of the crust: deformation-driven flow (Oliver 1996) and thermally driven flow (i.e., buoyancy-driven) through the crust, which is favoured by the high (1) permeability of detachments that collect and bring up deep hot fluids and (2) temperature induced by the shear heating mechanism. This latter term refers to the generation of heat from the mechanical work of tectonic processes (Scholz 1980). It thus increases with slip rate, friction coefficient and stiffness of materials (Leloup et al. 1999; Souche et al. 2013). Considered as a most rapidly deforming regions (e.g., Reilinger et al. 2006), western Anatolia domain would favour the development of such mechanism at crustal scale.

Fig. 12 Conceptual models at different scales showing the heat source origin and main structural controls on fluid flows in the Menderes Massif. **a** Synthetic simplified block diagram at basin scale showing the relationships between these faults. Numbers show different type of faults. Geothermal features and fluid circulation are also indicated. **b** Role of the detachment on deep circulation in the Menderes Massif. Main structures and flow directions in the mantle are indicated in abbreviations: *AD* Alaşehir detachment, *BD* Büyük Menderes detachment, *SD* Simav detachment, *SMSZ* Southern Menderes shear zone. **c** Tentative 3D reconstruction and flow directions in the mantle (red arrows) of the Aegean region before the recent slab tear below the Corinth Rift and after. Red line and red arrows show the main detachments and kinematic of extension in this region, respectively. Yellow arrows indicate the slab retreat in the Aegean domain. Main structures are indicated in abbreviations: *AD* Alaşehir detachment, *BD* Büyük Menderes detachment, *NAF* North Anatolian Fault, *NCDS* North Cycladic Detachment System, *SD* Simav detachment



Indeed, neo-tectonic activity in the Menderes Massif is characterized by earthquakes occurring in the shallow crust, with the mean depth being shallower in the Simav domain (9.7 km) compared to the western domain (11.9 km) and the central Menderes (11.2 km) domain (Gessner et al. 2013). Brittle deformation is still active [e.g., the Gediz detachment, Buscher et al. (2013)] and may locally occur under high-temperature conditions (e.g., 580 °C at ~ 10 km, Bilim et al. 2016), probably close to the ductile–brittle transition

zone. The numerous ductile shear zones may have had (and perhaps still have; e.g., Ring et al. 2017) a strong and continuous thermal effect at depth, explaining also the anomalously shallow position of Curie-point depths. Hence, in these areas heat could also be generated by tectonic processes, probably along the brittle–ductile shear zones in the upper levels of the continental crust (Fig. 12b) (Scholz 1980). Although the contribution of shear heating at crustal scale is debated (Lachenbruch and Sass 1992), more studies

would be needed to explore this possibility. In particular, the amount of heat produced and the time constants of such heat production should be addressed.

Furthermore, using a numerical model of coupled fluid flow and heat transport processes, Magri et al. (2010) showed that temperature patterns in the Seferihisar-Balçova area result from both interaction of convective flow (i.e., buoyancy-driven flow) and meteoric recharge induced by the horst (i.e., mixed convection) in the shallower crust. Recently, Roche et al. (2018) showed that high temperatures at 6 km depth (300–350 °C) are sufficient to allow a high fluid density contrast, permitting upward flow along the low-angle fault, using also 2-D numerical models (see Fig. 8 in their study). This implies that buoyancy-driven flow is superimposed to topography-driven flow in some places. This case is, for instance, well observed in the Seferihisar geothermal systems, where the topographic gradient related to the formation of MCC appears to be negligible. This implies that the observed temperature patterns result mainly from the thermally driven flow within permeable faults. In all cases, hot fluids in the detachments will further enhance temperature increase in the upper part of the fault zone, thus generating high thermal gradients in these

areas. For instance, Gottardi et al. (2011) estimated high-temperature gradient of ~ 140 °C/100 m across the Miocene Raft River shear zone in the United States, as revealed by isotope thermometry. There, the geotherm is quasi-stable over a long time duration. As a consequence, it raises the question whether similar geothermal fields in the Menderes Massif could have been active during millions of years.

In addition, it is clear that permeability related to fault zones architecture is a first-order control on fluid flow in the upper crust (e.g., Caine et al. 1996). Our study shows that the thick siliceous microbreccia of the Alaşehir detachment fault plane (Table 2) acts as cap fault of the fluid circulating below this plane. Thus, depending on the area, the detachment can be considered at kilometeric scale as a combined “conduit-barrier” and as a “localized conduit” (Caine et al. 1996), where the conduit corresponds to the thick shear zone and the barrier is associated with the fault plane and/or with the hanging wall of the detachment. Depending on the pressure gradients, the flow within the detachment may be characterized by horizontal-flow according to normal kinematic and related dilatancy (Fig. 12a). In both cases, the high permeability in the shear zone favours fluid circulation (e.g., in marbles levels through karstification process in the

Table 2 Main controls on geothermal fields in the Menderes Massif

	Geothermal fields	Structural setting	Structural characteristics	Main controls
Alaşehir graben	Salihli	HW and FW of the south side of the graben	Intersections between N-dipping detachment, N–S trending strike-slip faults and sometimes E–W trending normal faults	KC, FC, FRC
	Alaşehir	HW and FW of the south side of the graben	Intersections between N-dipping detachment, N–S trending strike-slip faults and sometimes E–W trending normal faults	
	Urganlı-Turgutlu	HW and FW of the north side of the graben	Intersections between N-dipping detachment, N–S trending strike-slip faults in the basin	FC
Büyük Menderes graben	Germencik	HW and FW of the north side of the graben	Intersections between S-dipping detachment, N–S trending strike-slip faults and E–W trending normal faults	FC, FRC
	Salavatlı	HW and FW of the north side of the graben	Intersections between NNE–SSW trending strike-slip faults and SE–NW striking normal faults	
	Kızıldere	HW and FW of the north side of the graben	Eastern termination of major normal fault; Intersections between N–S trending strike-slip faults and E–W striking normal fault	
Cumaovası basin	Seferihisar	HW and FW of the contact between BM/MU	Intersections between N–S transfer faults and the contact between BM/MU	FC
Simav graben	Simav	HW and FW of the north side of the graben	N-dipping detachment and intersections between N–S striking transfer fault and S-dipping normal fault	FC

BD Büyük Menderes detachment, *BM* Bornova Mélange, *FC* Fault controlled, *FRC* Fracture controlled, *FW* Foot wall, *AD* Alaşehir detachment, *HW* Hanging wall, *KC* Karstic controlled, *MU* Menderes Unit, *NF* Normal fault

Menderes Massif) and thus generates secondary reservoirs (Fig. 12a).

Basin scale: the N–S transfer faults

Based on our structural observations, we highlight that strike-slip faults control many geothermal reservoirs in depth, related to hot springs and travertine deposits at the surface. In terms of geometry, for instance, Çiftçi and Bozkurt (2010) suggested, from a seismic profile interpretation, the existence of two kilometric transfer faults with a large normal component in the Alaşehir graben (Fig. 4a). These transfer faults correspond to the location of several travertines oriented NW–SE and NE–SW and hot springs at the surface, which are, respectively, associated with the Urganlı (Temiz and Eikenberg 2011) and Alaşehir geothermal field (Fig. 4a). Kaya (2015) also suggests that the Tekkehamam geothermal field (located in the southern part of the Büyük Menderes graben, Fig. 1b) is associated with an N–S transfer fault that cuts both the basement and Neogene sediments. Thus, this set of faults is a good candidate to act as conduit for fluid circulation when hot springs and related travertines are located far from the detachment (Fig. 12a; Table 2). Here, horse-tail termination of these strike-slip faults (see more details in Faulds et al. 2011), generates many closely spaced faults that locally increase permeability, favouring the growth of reservoirs.

Although no clear chronology between detachments and the N–S strike-slip transfer zones can be observed in the field, we favour a contemporaneous and ongoing development of these faults systems during the development of the sedimentary basin according to Oner and Dilek (2013). They are mainly found at the foothills of the main Menderes mountains, crosscutting the detachments in high topographic zones. Nonetheless, we suggest that these faults may also root to detachments at deeper depth (Fig. 12a). There, pull-apart structures, *en échelon* and relay-ramp faults may be locally developed, generating dilational jogs with vertical pitch that focus fluid circulation and thus geothermal upflow (Figs. 6d, 11c). In addition, reservoirs are commonly focused at the dilational junction between detachments and nearby N–S strike-slip faults or within the strike-slip faults (e.g., Cumalı fault, Figs. 11a, 12a).

To sum-up, these faults define several 100 m wide relay zones, where faults are considered as “distributed conduits” (Caine et al. 1996). They are characterized by multiple minor faults, connected with major structures, where fluids can flow through highly fractured metamorphic rocks thanks to the seismic pumping mechanism (e.g., Sibson et al. 1975; McCaig 1988; Famin et al. 2005). Consequently, we refer hereafter to these sinistral or dextral strike-slip faults as the “geothermal transverse and transfer faults” related to main reservoirs (Fig. 12a). Hence, these faults should be used as

a main guide for geothermal exploration. This hypothesis is opposed to the idea of Gessner et al. (2017), suggesting that NNE–SSW-orientated lineaments do not have a significant role in fluid flow pattern.

Possible fluid pathways in the Menderes Massif: from the mantle to the geothermal reservoir

In this study we have emphasized two types of control on hot springs and related geothermal fluid flow in the Alaşehir, Büyük Menderes and Cumaovası basins: a structural control and a lithological control (Table 2), which is also determinant to understand the location of hot springs and to explain the position of reservoirs at depth. In the following, we first propose a fluid pathway at the scale of the Menderes Massif (Fig. 12a) and then we mention a possible long-live duration for this type of systems.

Source to sink

Based on structural analyses of field data and isotopic distribution of waters, we suggest similar pathways of fluids for the Alaşehir and the Büyük Menderes half-grabens, that could also extend to the Simav graben and Cumaovası basin: meteoric cold waters and/or sea waters (i.e., for the Seferhisar case) circulate downwards along E–W high-angle to listric normal faults (e.g., Salihli and Alaşehir geothermal systems), implying that such faults control the meteoric recharge of deeper reservoirs (Fig. 12a). More generally, meteoric water infiltration along fractured rocks of the basement of the Menderes Massif is controlled by (1) the foot-wall topography gradient induced by MCC exhumation, and by (2) the stress regime in the crust, allowing recharge and hydrothermal fluid circulation. Then, temperature of fluids increases progressively. Hot fluids can circulate along the main detachments (i.e., Simav, Alaşehir and Büyük Menderes detachments) related to karstified marbles or/ in fractured rocks of the basement. During this stage, the geochemical properties of meteoric waters are modified and their composition (e.g., Na–HCO₃ type) is mainly controlled by calcite dissolution in the marbles layers of the Menderes Massif under high-temperature conditions. Locally, some exchange with mantle–He, CO₂, B and H₂S isotopes could occur in deep parts of the crust in the ductile–brittle transition zone (Fig. 12b). Through a seismic pumping mechanism (e.g., Sibson et al. 1975; McCaig 1988; Famin et al. 2005), hydraulic gradients may force fluid downward across the ductile–brittle transition using the high permeability of microcrack networks (e.g., after earthquake rupture). After a complex deep fluid pathway, thermal waters may then recharge reservoirs of the metamorphic rocks of the Menderes at depth (Fig. 12a, b).

Different lithologies may behave as reservoirs (Table 1). Reservoirs are herein defined by highly fractured but also by karstified carbonate layers of the CMM (e.g., Salihli, Alaşehir, Germencik, Salavatlı...; Tarcan et al. 2000). For instance, the high-temperature geothermal reservoir observed in Alaşehir, is located in the upper section of the Paleozoic basement, with feeder zones in the upper Paleozoic carbonates at approximately 1150 m and 1600 m of depth (Akin et al. 2015). Fractured metamorphic rocks such as quartzite can also act as an aquifer for geothermal fluid (e.g., Kızıldere; Simsek 2003). In both cases, the main reservoirs are located just below the detachments, which is in some places silicified (Fig. 12a). There, blind geothermal reservoirs may also form. Indeed, according to Magri et al. (2010), when hydrothermal plumes reach the upper impermeable boundary (e.g., the Alaşehir detachment), over-pressured blind geothermal reservoirs are formed. This implies that other geothermal systems in the Menderes Massif are yet to be discovered. To fully understand these geothermal systems, stress modelling related to faulting is necessary to bring new constraints on the evolution of fluid pathways (Moeck et al. 2009). In addition, other reservoir types may be developed in the hanging wall of detachments. For example, in the Cumaovası basin, it is made of fractured submarine volcanics of the Bornova mélangé (Tarcan and Gemici 2003). Because of the high permeability units in Neogene continental silicoclastic rocks, secondary aquifers may also occur (Fig. 12a). Indeed, Neogene sediments may have highly variable permeability, but they usually rather display mega-cap rocks related to underlying geothermal system (Tarcan et al. 2000; e.g., the Alaşehir geothermal system).

After a short time of residence (around 20–50 years, Simsek 2003) in different kinds of reservoirs, hot thermal fluids can flow along the dilational intersections or junction between the N–S strike-slip faults and the detachment, and then emerge at the surface (e.g., Kurşunlu, Sart-Çamur, Germencik hot springs) (Fig. 12a). In this case, the direction of flow is mainly determined by the prevailing permeability and by the regional stress field. Similar features of fluid flow pattern are observed in the Cumaovası basin, where the NE–SW trending strike-slip faults affected also the detachment, forming dilational jogs and favouring hot water circulation from karstic and fractured reservoirs to the surface (e.g., Fig. 11b, c).

A long-lived duration geothermal Province?

Hetzl et al. (2013) suggested that the Alaşehir and Büyük Menderes detachments recorded a long-lived brittle deformation from around 22 Ma until 4–3 Ma. Hence, the low-angle crustal normal faults were (still) active over a long period of time. We thus suggest that detachments controlled magma ascent (e.g., Salihli granodiorite, Egrigöz granite)

as well as fluid circulation in the Menderes Massif during the Miocene. Nonetheless, the presence of Kursunlu Sb–Hg(–Au) deposit (Larson and Erler 1993) located within the Alaşehir detachment system, implies a drastic change in the fluid pathway evolution compare to the Miocene. Indeed, according to Larson and Erler (1993), Alaşehir detachment conveyed deep circulation of shallow hydrothermal fluids (i.e., meteoric origin) with a minor component of crustal and mantellic origin, thus similar to the present-day hot springs. Hence, the mineralizing fluid seems to be not related to the Miocene intrusions. To better characterize this evolution, a detailed study of such deposit would be useful, bringing new constraints on the structural control of the mineralization and the timing of mineralizing processes. This imply that detachments control fluid pathways over millions years (episodic or continuous mineralized pulse(s)?).

Origin of heat source in the Menderes Massif

At geodynamic scale, the origin of the thermal anomalies propagating all the way to the surface could reflect both slab rollback and slab tear below western Turkey. Heat can be generated by many processes, including anomalous mantle heat flow mainly due to asthenospheric flow and shear heating (Fig. 12c) (Roche et al. 2018). Based on heat conduction, the time scale t_{diff} is defined by the following equation:

$$t_{\text{diff}} = L^2 / \kappa, \quad (1)$$

where L is Moho depth (meter) and κ is the thermal diffusivity ($\text{m}^2 \text{s}^{-1}$). Considering a Moho depth of ~ 25 km under the Menderes Massif (e.g., Karabulut et al. 2013) and taking a thermal diffusivity (κ) of $10^{-6} \text{ m}^2 \text{ s}^{-1}$, the current thermal anomaly observed at the surface (shown by the presence of numerous sources and gas events) could reflect the thermal expression of a 20 Ma old slab tear at Moho depth. In other words, the heat source at the base of the crust coupled to the exhumation of the MCC is induced by slab dynamics since the Miocene as suggested by previous authors (e.g., Jolivet et al. 2015; Menant et al. 2016, 2018; Roche et al. 2018). This increase of temperature recorded in the mantle and in the crust favours the emplacement of a large zone of migmatization and/or magmatic underplating at the base of the crust. This hypothesis is also consistent with:

1. the presence of high temperatures (~ 580 °C) at shallow depths (~ 10 km under the Menderes; Aydin et al. 2005; Bilim et al. 2016);
2. the current models of Miocene slab tearing in this region (Jolivet et al. 2015).
3. the enrichment of mantle–He (Mutlu et al. 2008), B and sometimes high content of CO_2 and H_2S within all thermal waters (Vengosh et al. 2002); for instance, mantle–He values suggest that helium is probably transferred

to the lower crust by degassed fluids from deep mantle melts (Mutlu et al. 2008); these values comparable to that observed in hydrothermal fluids from the western part of the Basin and Range Province (4–25% mantle–He), where active volcanism is also absent (Kennedy and Soest 2007).

To sum-up, the lack of significant magmatic activity in this area shows that the upper crust and related magmatic bodies is not a direct heat source for these geothermal systems (Faulds et al. 2010). Nevertheless, based on 3-D Vp imaging of the upper crust beneath the Denizli geothermal field, Kaypak and Gökkaya (2012) showed that intrusive magmatic bodies may also explain the heat source of few geothermal systems in this area. According to this study and others (e.g., Faulds et al. 2010; Kaya 2015; Gessner et al. 2017) the spatial distribution of hot springs and fumaroles is associated with the tectonic activity. Using the classification of Moeck (2014), the “geothermal Province” of the Menderes Massif can be considered as a fault-controlled system in an extensional domain, where convection occurs along the transfer fault systems. Although most of existing models of geothermal heat source suggest a probable magmatic intrusion in the upper crust, this study argues that the tectonic activity induced by subduction dynamics controls the spatial distribution of heat in the Menderes massif (Fig. 12c) (e.g., Kaya 2015; Gessner et al. 2017; Roche et al. 2018). We thus think that this area may be used as a reference case to better understand the amagmatic geothermal systems/Provinces.

An underestimated geothermal potential?

It is clear that dense fracturing caused by tectonic activity implies a modification of the regional fluid flow, which is controlled by the state of stress in the crust, and influences the localisation and the typology of reservoirs. Reilinger et al. (2006) have estimated fault-slip rates in a block model consisting of 19 plates/blocks and using $M > 4.5$ earthquakes above 35 km. Based on GPS-derived velocity field data, they suggested a total extension of approximately 25 mm/year corresponding to 10.9 ± 0.3 mm/year for the left-lateral strike-slip component and 14.5 ± 0.3 mm/year of pure extension. This rapid relative motion is twice the rate reported from the Basin and Range Province, where Bennett et al. (2003) estimate relative motion of 9.3 ± 0.2 mm/year with high strain rates, using the same method (i.e., GPS-derived velocity field data). Faulds et al. (2012) showed that the regional pattern of geothermal activity in the same area is directly correlated with strain rates. If we compare, for instance, the total discharge of the Seferihisar geothermal field [e.g., 100–150 L/s to 300 L/s according to Tarcan and Gemici (2003)], located in a seismically active zone (e.g., see compilation from Özkaymak et al. 2013) is twice to four

times that of the Salihli geothermal field (2–80 L/s; Özen et al. 2012), which is a less active zone. Paradoxically, the topography is less steep in Seferihisar area than in Salihli area. Therefore, we suggest that active deformation could affect fluid velocity in the upper crust, improving the flow rates of a geothermal system.

Furthermore, the Basin & Range Province is quite similar to the Menderes Province, because MCCs are exhumed along low-angle normal faults, and represent a favourable setting for amagmatic high-enthalpy geothermal resources (Roche et al. 2018). In addition, the origin of the heat of these systems may be also associated with a deeper source induced by subduction dynamics (i.e., magmatic underplating under the overriding plate; Wannamaker et al. 2006). Because of the similarities between these both geothermal Provinces, we suggest that the geothermal potential in the Menderes is probably underestimated (~820 MWe, Geothermal Resource Association estimated in 2018). Indeed, the current geothermal installed capacity of the Basin and Range province is estimated at ~2349 MWe (Bertani 2016).

Conclusion

Our work is based on a multi-scale study and on a compilation of geothermal and structural observations in the whole Menderes Massif. It provides a new vision on the role of a large-scale thermal anomaly below the Menderes Massif and more generally in the Eastern Mediterranean region. We suggest that such regional thermal anomalies at the origin of the Menderes geothermal Province result from the tectono-thermal evolution of the Aegean subduction zone at depth. This Province is characterized by an intense hydrothermal activity, favoured by both a high elevation area and a neotectonic activity in absence of magmatic input. Such proxies are related to the Menderes Core Complex evolution, which is structured by three main detachments. We also have identified, at crustal scale, the essential role of the low-angle normal faults, corresponding to a permeable channelized fluid flow systems for ascending fluid flows. N–S transfer faults then control the position of geothermal systems and should be used as a main guide for geothermal exploration. In addition, we emphasize that the lithological control is determinant for understanding the location of geothermal reservoirs, and may have a strong influence in the fluid circulation pattern of thermal waters. Eventually, we highlight that an episodic model (e.g., seismic pumping) and / or a continuous model seem possible over several million years in the Menderes Massif.

Acknowledgements This work has received funding from the Labex Voltaire (ANR-10-LABX-100-01) homed at Orléans University and BRGM, the French geological survey. The paper benefited from

relevant revisions by Inga Moeck, Klaus Gessner and Gürol Seyitoğlu. We also thank the Editor in chief, Wolf-Christian Dullo.

References

- Akin S, Yildirim N, Yazman M, Karadag M, Seçkin C, Tonguç E, Gürel E, Yarım H (2015) Coiled tubing acid stimulation of alaşehir geothermal field, Turkey. In: Proceedings world geothermal congress 2015, Melbourne, Australia, 19–25 April 2015
- Akkus I, Akıllı H, Ceyhan S, Dilemre A, Tekin Z (2005) Türkiye jeotermal kaynakları envanteri. MTA Genel Müdürlüğü Yayınları, Envanter Serisi, 201
- Alçıçek H, Bülbül A, Brogi A, Liotta D, Ruggieri G, Capezzuoli E et al (2018) Origin, evolution and geothermometry of the thermal waters in the Gölemezli Geothermal Field, Denizli Basin (SW Anatolia, Turkey). *J Volcanol Geoth Res* 349:1–30
- Altinoğlu FF, Sari M, Aydın A (2015) Detection of lineaments in denizli basin of western Anatolia region using bouguer gravity data. *Pure Appl Geophys* 172:415–425
- Andritsos N, Dalambakis P, Arvanitis A, Papachristou M, Fytikas M (2015) Geothermal developments in Greece—Country update 2010–2014. In: Proceedings world geothermal congress 2015, pp 19–24
- Asti R (2016) A source-to-sink history of the supradetachment gediz graben (W Turkey): from exhumation of the central Menderes Massif through the Gediz detachment fault to sedimentation in the basin, ArcAdiA
- Aydın İ, Karat H, Koçak A (2005) Curie-point depth map of Turkey. *Geophys J Int* 162(2):633–640
- Baba A, Bundschuh J, Chandrasekharan D (eds) (2014) Geothermal systems and energy resources: Turkey and Greece. CRC, Boca Raton
- Baba A, Şimşek C, Gündüz O, Elçi A, Murathan A (2015) Hydrogeochemical properties of geothermal fluid and its effect on the environment in Gediz Graben, Western Turkey. In: Proceedings world geothermal congress 2015, Melbourne, Australia, 19–25 April 2015
- Bayrak M, Serpen Ü, İlkışık OM (2011) Two-dimensional resistivity imaging in the Kızıldere geothermal field by MT and DC methods. *J Volcanol Geotherm Res* 204:1–11
- Bayram AF, Simsek S (2005) Hydrogeochemical and isotopic survey of Kütahya-Simav geothermal field. In: Proceedings of world geothermal congress, Antalya, Turkey, pp 24–29
- Bennett RA, Wernicke BP, Niemi NA, Friedrich AM, Davis JL (2003) Contemporary strain rates in the northern Basin and Range province from GPS data. *Tectonics*. <https://doi.org/10.1029/2001TC001355>
- Benoit D (1999) Conceptual models of the Dixie Valley, Nevada geothermal field. *Trans Geotherm Resour Council* 1999:505–512
- Bertani R (2016) Geothermal power generation in the world 2010–2014 update report. *Geothermics* 60:31–43
- Bilim F, Akay T, Aydemir A, Kosaroglu S (2016) Curie point depth, heat-flow and radiogenic heat production deduced from the spectral analysis of the aeromagnetic data for geothermal investigation on the Menderes Massif and the Aegean Region, western Turkey. *Geothermics* 60:44–57
- Biryol CB, Beck SL, Zandt G, Özacar AA (2011) Segmented African lithosphere beneath the Anatolian region inferred from teleseismic P-wave tomography. *Geophys J Int* 184:1037–1057
- Blackwell DD, Golan B, Benoit D (2000) Thermal regime in the Dixie Valley geothermal system. *Geotherm Resour Council Trans* 24:223–228
- Bonneau M, Kienast JR (1982) Subduction, collision et schistes bleus: exemple de l'Égée. *Grèce Bull Soc Géol France* 7:785–791
- Bozkurt E (2001) Late Alpine evolution of the central Menderes Massif, western Turkey. *Int J Earth Sci* 89:728–744. <https://doi.org/10.1007/s005310000141>
- Bozkurt E, Oberhänsli R (2001) Menderes Massif (Western Turkey): structural, metamorphic and magmatic evolution—a synthesis. *Int J Earth Sci* 89:679–708
- Bozkurt E, Sözbilir H (2004) Tectonic evolution of the Gediz Graben: field evidence for an episodic, two-stage extension in western Turkey. *Geol Mag* 141:63–79
- Bozkurt E, Satır M, Buğdaycıoğlu Ç (2011) Surprisingly young Rb/Sr ages from the Simav extensional detachment fault zone, northern Menderes Massif, Turkey. *J Geodyn* 52:406–431
- Buck WR (1988) Flexural rotation of normal faults. *Tectonics* 7(5):959–973
- Bülbül A, Özen T, Tarcan G (2011) Hydrogeochemical and hydrogeological investigations of thermal waters in the Alasehir-Kavaklıdere area (Manisa-Turkey). *Afr J Biotechnol* 10:17223–17240
- Bunbury JM, Hall L, Anderson GJ, Stannard A (2001) The determination of fault movement history from the interaction of local drainage with volcanic episodes. *Geol Mag* 138(2):185–192
- Buscher JT, Hampel A, Hetzel R, Dunkl I, Glotzbach C, Struffert A et al (2013) Quantifying rates of detachment faulting and erosion in the central Menderes Massif (western Turkey) by thermochronology and cosmogenic ¹⁰Be. *J Geol Soc* 170(4):669–683
- Caine JS, Evans JP, Forster CB (1996) Fault zone architecture and permeability structure. *Geology* 24(11):1025–1028
- Çifçi G, Pamukçu O, Çoruh C, Çopur S, Sözbilir H (2011) Shallow and deep structure of a supradetachment basin based on geological, conventional deep seismic reflection sections and gravity data in the Buyuk Menderes Graben, western Anatolia. *Surv Geophys* 32(3):271–290
- Çiftçi NB, Bozkurt E (2009) Pattern of normal faulting in the Gediz Graben, SW Turkey. *Tectonophysics* 473(1–2):234–260
- Çiftçi NB, Bozkurt E (2010) Structural evolution of the Gediz Graben, SW Turkey: temporal and spatial variation of the graben basin. *Basin Res* 22:846–873
- Collins AS, Robertson AHF (1998) Processes of Late Cretaceous to Late Miocene episodic thrust-sheet translation in the Lycian Taurides, SW Turkey. *J Geol Soc* 15:759–772
- De Boorder H, Spakman W, White SH, Wortel MJR (1998) Late Cenozoic mineralization, orogenic collapse and slab detachment in the European Alpine Belt. *Earth Planet Sci Lett* 164(3):569–575
- Delvaux D, Sperner B (2003) New aspects of tectonic stress inversion with reference to the TENSOR program. *Geol Soc Lond Spec Publ* 212(1):75–100
- Demircioğlu D, Ecevitoglu B, Seyitoğlu G (2010) Evidence of a rolling hinge mechanism in the seismic records of the hydrocarbon-bearing Alaşehir graben, western Turkey. *Pet Geosci* 16(2):155–160
- Dercourt J, Zonenshain LP, Ricou LE, Kuzmin VG, Le Pichon X, Knipper AL, Grandjacquet C, Sbertshikov IM, Geyssant J, Lepvrier C, Pechersky DH, Boulain J, Sibuet JC, Savostin LA, Sorokhtin O, Westphal M, Bazhenov ML, Lauer JP, Biju-Duval B (1986) Geological evolution of the Tethys belt from the Atlantic to the Pamir since the Lias. *Tectonophysics* 123:241–315
- Dilek Y, Altunkaynak Ş (2009) Geochemical and temporal evolution of Cenozoic magmatism in western Turkey: mantle response to collision, slab break-off, and lithospheric tearing in an orogenic belt. *Geol Soc Lond Spec Publ* 311:213–233
- Dolmaz MN, Ustaömer T, Hisarlı ZM, Orbay N (2005) Curie point depth variations to infer thermal structure of the crust at the African-Eurasian convergence zone, SW Turkey. *Earth Planets Sp* 57(5):373–383
- Dora O, Kun N, Candan O (1990) Metamorphic history and geotectonic evolution of the Menderes Massif. *IIESCA Proc* 2:102–115

- Drahor MG, Berge MA (2006) Geophysical investigations of the Seferihisar geothermal area, Western Anatolia. *Turk Geotherm* 35:302–320
- Emre T (1992) Gediz grabeni'nin (Salihli-Alaflehir arasi) jeolojisi. 45. Türkiye Jeoloji Kurultayı Bildiri Ozleri, s.60
- Emre T, Sözbilir H (1997) Field evidence for metamorphic core complex, detachment faulting and accommodation faults in the Gediz and Büyük Menderes grabens, western Anatolia. In: International earth sciences colloquium on the Aegean Region, Izmir-Güllük, Turkey. pp 73–93
- Endrun B, Lebedev S, Meier T, Tirel C, Friederich W (2011) Complex layered deformation within the Aegean crust and mantle revealed by seismic anisotropy. *Nat Geosci* 4(3):203
- Epstein S, Sharp RP, Gow AJ (1965) Six-year record of oxygen and hydrogen isotope variations in South Pole firn. *J Geophys Res* 70(8):1809–1814
- Erdoğan B (1990) İzmir-Ankara Zonu'nun, İzmir ile Seferihisar arasındaki bölgede stratigrafik özellikleri ve tektonik evrimi. *TPJD Bül* 2:1–20
- Erkan K (2014) Crustal heat flow measurements in western Anatolia from borehole equilibrium temperatures. *Solid Earth Discuss* 6:403–426
- Erkan K (2015) Geothermal investigations in western Anatolia using equilibrium temperatures from shallow boreholes. *Solid Earth* 6(1):103
- Ersoy EY, Helvacı C, Palmer MR (2010) Mantle source characteristics and melting models for the early-middle Miocene mafic volcanism in Western Anatolia: implications for enrichment processes of mantle lithosphere and origin of K-rich volcanism in postcollisional settings. *J Volcanol Geotherm Res* 198:112–128
- Faccenna C, Piromallo C, Crespo-Blanc A, Jolivet L, Rossetti F (2004) Lateral slab deformation and the origin of the Western Mediterranean arcs. *Tectonics*. <https://doi.org/10.1029/2002T C001488>
- Faccenna C, Bellier O, Martinod J, Piromallo C, Regard V (2006) Slab detachment beneath eastern Anatolia: a possible cause for the formation of the North Anatolian fault. *Earth Planet Sci Lett* 242(1–2):85–97
- Famin V, Philippot P, Jolivet L, Agard P (2004) Evolution of hydrothermal regime along a crustal shear zone, Tinos Island, Greece. *Tectonics* 23:5
- Famin V, Hébert R, Philippot P, Jolivet L (2005) Ion probe and fluid inclusion evidences for co-seismic fluid infiltration in a crustal detachment. *Contrib Mineral Petrol* 150(3):354–367. <https://doi.org/10.1007/s00410-005-0031-x>
- Faulds JE, Coolbaugh M, Blewitt G, Henry CD (2004) Why is Nevada in hot water? Structural controls and tectonic model of geothermal systems in the northwestern Great Basin. *Geotherm Resour Council Trans* 28:649–654
- Faulds J, Coolbaugh M, Bouchot V, Moek I, Oguz K (2010) Characterizing structural controls of geothermal reservoirs in the Great Basin, USA, and Western Turkey: developing successful exploration strategies in extended terranes. In: Presented at the world geothermal congress 2010, p 11
- Faulds JE, Hinz NH, Coolbaugh MF, Cashman PH, Kratt C, Dering G et al (2011) Assessment of favorable structural settings of geothermal systems in the Great Basin, western USA. *Geotherm Resour Council Trans* 35:777–783
- Faulds JE, Hinz N, Kreemer C, Coolbaugh M (2012) Regional patterns of geothermal activity in the Great Basin Region, Western USA: correlation with strain rates. *Geotherm Resour Council Trans* 36:897–902
- Filiz S, Tarcan G, Gemici U (2000) Geochemistry of the Germencik geothermal fields, Turkey. In: Proceedings of the world geothermal congress, pp 1115–1120
- Gemici Ü, Tarcan G (2002) Hydrogeochemistry of the Simav geothermal field, western Anatolia, Turkey. *J Volcanol Geoth Res* 116(3–4):215–233
- Genç C, Altunkaynak Ş, Karacık Z, Yazman M, Yılmaz Y (2001) The Çubukludağ graben, south of İzmir: its tectonic significance in the Neogene geological evolution of the western Anatolia. *Geodin Acta* 14(1–3):45–55
- Gessner K, Piazzolo S, Güngör T, Ring U, Kröner A, Passchier CW (2001a) Tectonic significance of deformation patterns in granitoid rocks of the Menderes nappes, Anatolide belt, southwest Turkey. *Int J Earth Sci* 89:766–780
- Gessner K, Ring U, Johnson C, Hetzel R, Passchier CW, Güngör T (2001b) An active bivergent rolling-hinge detachment system: central Menderes metamorphic core complex in western Turkey. *Geology* 29:611–614
- Gessner K, Gallardo LA, Markwitz V, Ring U, Thomson SN (2013) What caused the denudation of the Menderes Massif: review of crustal evolution, lithosphere structure, and dynamic topography in southwest Turkey. *Gondwana Res* 24(1):243–274
- Gessner K, Markwitz V, Güngör T (2017) Crustal fluid flow in hot continental extension: tectonic framework of geothermal areas and mineral deposits in western Anatolia. *Geol Soc Lond Spec Publ* 453:SP453–S7
- Gottardi R, Teysseier C, Mulch A, Vennemann TW, Wells ML (2011) Preservation of an extreme transient geotherm in the Raft River detachment shear zone. *Geology* 39(8):759–762
- Govers R, Fichtner A (2016) Signature of slab fragmentation beneath Anatolia from full-waveform tomography. *Earth Planet Sci Lett* 450:10–19. <https://doi.org/10.1016/j.epsl.2016.06.014>
- Govers R, Wortel MJR (2005) Lithosphere tearing at STEP faults: response to edges of subduction zones. *Earth Planet Sci Lett* 236:505–523
- Güleç N (1988) Helium-3 distribution in western Turkey. *Miner Res Expl Bull* 108:35–42
- Güleç N, Hilton DR (2006) Helium and heat distribution in western Anatolia, Turkey: relationship to active extension and volcanism. *Geol Soc Am Spec Pap* 409:305–319
- Güleç N, Hilton DR, Mutlu H (2002) Helium isotope variations in Turkey: relationship to tectonics, volcanism and recent seismic activities. *Chem Geol* 187:129–142
- Güngör T, Erdoğan B (2002) Tectonic significance of mafic volcanic rocks in a Mesozoic sequence of the Menderes Massif, West Turkey. *Int J Earth Sci* 91(3):386–397
- Haizlip JR, Haklıdır FT, Garg SK (2013) Comparison of reservoir conditions in high noncondensable gas geothermal systems. In: Proceedings, 38th workshop on geothermal reservoir engineering, pp 11–13
- Haklıdır FT, Sengun R, Haizlip JR (2015) The geochemistry of the deep reservoir wells in Kizildere (Denizli City) geothermal field (Turkey). *Geochemistry* 19:25
- Hetzel R, Passchier CW, Ring U, Dora ÖO (1995a) Bivergent extension in orogenic belts: the Menderes Massif (southwestern Turkey). *Geology* 23:455–458
- Hetzel R, Ring U, Akal C, Troesch M (1995b) Miocene NNE-directed extensional unroofing in the Menderes Massif, southwestern Turkey. *J Geol Soc* 152:639–654
- Hetzel R, Zwingmann H, Mulch A, Gessner K, Akal C, Hampel A, Güngör T, Petschick R, Mikes T, Wedin F (2013) Spatiotemporal evolution of brittle normal faulting and fluid infiltration in detachment fault systems: a case study from the Menderes Massif, western Turkey. *Tectonics* 32:364–376
- Isik V, Tekeli O, Cemen I (1997) Mylonitic fabric development along a detachment surface in northern Menderes massif, western Anatolia, Turkey. In: Geol. Soc. America, abstracts with programs
- Isik V, Tekeli O, Seyitoglu G (2004) The 40Ar/39Ar age of extensional ductile deformation and granitoid intrusion in the

- northern Menderes core complex: implications for the initiation of extensional tectonics in western Turkey. *J Asian Earth Sci* 23(4):555–566
- Işık V, Tekeli O (2001) Late orogenic crustal extension in the northern Menderes Massif (western Turkey): evidence for metamorphic core complex formation. *Int J Earth Sci* 89:757–765
- Işık V, Seyitoğlu G, Cemen I (2003) Ductile–brittle transition along the Alaşehir detachment fault and its structural relationship with the Simav detachment fault, Menderes Massif, western Turkey. *Tectonophysics* 374:1–18
- Jolie E, Klinkmueller M, Moeck I, Bruhn D (2016) Linking gas fluxes at Earth's surface with fracture zones in an active geothermal field. *Geology*, G37412-1
- Jolivet L, Brun JP (2010) Cenozoic geodynamic evolution of the Aegean. *Int J Earth Sci Geol Rundsch* 99(6):109–138. <https://doi.org/10.1007/s00531-008-0366-4>
- Jolivet L, Faccenna C (2000) Mediterranean extension and the Africa–Eurasia collision. *Tectonics* 19:1095–1106. <https://doi.org/10.1029/2000TC900018>
- Jolivet L, Goffé B, Monié P, Truffert-Luxey C, Patriat M, Bonneau M (1996) Miocene detachment in Crete and exhumation P-T-t paths of high-pressure metamorphic rocks. *Tectonics* 15:1129–1153
- Jolivet L, Faccenna C, Huet B, Labrousse L, Le Pourhiet L, Lacombe O et al (2013) Aegean tectonics: strain localisation, slab tearing and trench retreat. *Tectonophysics* 597:1–33
- Jolivet L, Menant A, Sternai P, Rabillard A, Arbaret L, Augier R, Laurent V, Beaudoin A, Grasemann B, Huet B, Labrousse L, Le Pourhiet L (2015) The geological signature of a slab tear below the Aegean. *Tectonophysics* 659:166–182. <https://doi.org/10.1016/j.tecto.2015.08.004>
- Jongsma D (1974) Heat flow in the Aegean Sea. *Geophys J Int* 37(3):337–346
- Karabulut H, Paul A, Afacan Ergün T, Hatzfeld D, Childs DM, Aktar M (2013) Long-wavelength undulations of the seismic Moho beneath the strongly stretched Western Anatolia. *Geophys J Int* 194:450–464. <https://doi.org/10.1093/gji/ggt1100>
- Karakuş H (2015) Helium and carbon isotope composition of gas discharges in the Simav Geothermal Field, Turkey: implications for the heat source. *Geothermics* 57:213–223
- Karamandereci İH (1997) Salihli-Caferbey (Manisa İli) jeotermal sahası potansiyelive geleceği. *Dunya Enerji Konseyi Turk Milli Komitesi, Türkiye 7. Enerji Kongresi teknik oturum bildiri metinleri*, pp 247–261 (in Turkish)
- Karamandereci İH (2013) Characteristics of geothermal reservoirs in Turkey. IGA Academy Report 0102-2013
- Karamandereci İH, Helvacı C (2003) Geology and hydrothermal alteration of the AydıN–Salavatlı geothermal field, western Anatolia, Turkey. *Turk J Earth Sci* 12:175–198
- Kaya A (2015) The effects of extensional structures on the heat transport mechanism: an example from the Ortakçı geothermal field (Büyük Menderes Graben, SW Turkey). *J Afr Earth Sci* 108:74–88
- Kaypak B, Gökaya G (2012) 3-D imaging of the upper crust beneath the Denizli geothermal region by local earthquake tomography, western Turkey. *J Volcanol Geoth Res* 211:47–60
- Kennedy BM, Van Soest MC (2007) Flow of mantle fluids through the ductile lower crust: helium isotope trends. *Science* 318(5855):1433–1436
- Kennedy BM, Kharaka YK, Evans WC, Ellwood A, DePaolo DJ, Thordsen J et al (1997) Mantle fluids in the San Andreas fault system, California. *Science* 278(5341):1278–1281
- Kent E, Boulton SJ, Stewart IS, Whittaker AC, Alçiçek MC (2016) Geomorphic and geological constraints on the active normal faulting of the Gediz (Alaşehir) Graben, Western Turkey. *J Geol Soc* 2016:jgs2015-121
- Kindap A, Kaya T, Haklıdır FST, Bükülmez AA (2010) Privatization of kizildere geothermal power plant and new approaches for field and plant. In: *Proceedings world geothermal congress*
- Koçyigit A, Yusufoglu H, Bozkurt E (1999) Discussion on evidence from the Gediz Graben for episodic two-stage extension in western Turkey. *J Geol Soc Lond* 156:1240–1242
- Koçyigit A (2015) An overview on the main stratigraphic and structural features of a geothermal area: the case of Nazilli-Buharkent section of the Büyük Menderes Graben, SW Turkey. *Geodin Acta* 27(2–3):85–109
- Kose R (2007) Geothermal energy potential for power generation in Turkey: a case study in Simav, Kutahya. *Renew Sustain Energy Rev* 11(3):497–511
- Kulongsoski JT, Hilton DR, Izbicki JA (2005) Source and movement of helium in the eastern Morongo groundwater Basin: the influence of regional tectonics on crustal and mantle helium fluxes. *Geochimica et cosmochimica Acta* 69(15):3857–3872
- Lachenbruch AH, Saas JH (1992) Heat flow from Cajon Pass, fault strength, and tectonic implications. *J Geophys Res* 97:4995–5015
- Larson LT, Erler YA (1993) The epithermal lithochemical signature—a persistent characterization of precious metal mineralization at Kursunlu and Örencik, two prospects of very different geology in western Turkey. *J Geochem Explor* 47(1–3):321–331
- Leloup PH, Ricard Y, Battaglia J, Lacassin R (1999) Shear heating in continental strike-slip shear zones: model and field examples. *Geophys J Int* 136:19–40
- Lips AL, Cassard D, Sözbilir H, Yılmaz H, Wijbrans JR (2001) Multistage exhumation of the Menderes massif, western Anatolia (Turkey). *Int J Earth Sci* 89(4):781–792
- Maddy D, Veldkamp A, Demir T, van Gorp W, Wijbrans JR, van Hinsbergen DJJ et al (2017) The Gediz River fluvial archive: a benchmark for quaternary research in Western Anatolia. *Quatern Sci Rev* 166:289–306
- Magri F, Akar T, Gemici U, Pekdeger A (2010) Deep geothermal groundwater flow in the Seferihisar–Bağcıva area, Turkey: results from transient numerical simulations of coupled fluid flow and heat transport processes. *Geofluids* 10:388–405
- Malinverno A, Ryan WBF (1986) Extension in the Tyrrhenian Sea and shortening in the Apennines as result of arc migration driven by sinking of the lithosphere. *Tectonics* 5:227–245. <https://doi.org/10.1029/TC005i002p00227>
- Marty B, O'niions RK, Oxburgh ER, Martel D, Lombardi S (1992) Helium isotopes in Alpine regions. *Tectonophysics* 206(1):71–78
- McCaig AM (1988) Deep fluid circulation in fault zones. *Geology* 16(10):867–870
- Menant A, Jolivet L, Vrielynck B (2016) Kinematic reconstructions and magmatic evolution illuminating crustal and mantle dynamics of the eastern Mediterranean region since the late Cretaceous. *Tectonophysics* 675:103–140
- Menant A, Jolivet L, Tuduri J, Loiselet C, Bertrand G, Guillou-Frottier L (2018) 3D subduction dynamics: a first-order parameter of the transition from copper- to gold-rich deposits in the eastern Mediterranean region. *Ore Geol Rev* 94:118–135
- Mendrinis D, Choropanitis I, Polyzou O, Karytsas C (2010) Exploring for geothermal resources in Greece. *Geothermics* 39:124–137
- Moeck IS (2014) Catalog of geothermal play types based on geologic controls. *Renew Sustain Energy Rev* 37:867–882
- Moeck IS, Schandlmeier H, Holl GH (2009) The stress regime in a Rotliegend reservoir of the Northeast German Basin. *Int J Earth Sci* 98(7):1643–1654
- Mulch A, Teyssier C, Cosca MA, Chamberlain CP (2007) Stable isotope paleoaltimetry of Eocene core complexes in the North American Cordillera. *Tectonics*. <https://doi.org/10.1029/2006TC001995>

- Mutlu H, Güleç N, Hilton DR (2008) Helium–carbon relationships in geothermal fluids of western Anatolia. *Turk Chem Geol* 247:305–321
- O’neils RK, Oxburgh ER (1988) Helium, volatile fluxes and the development of continental crust. *Earth Planet Sci Lett* 90(3):331–347
- Oliver NHS (1996) Review and classification of structural controls on fluid flow during regional metamorphism. *J Metamorph Geol* 14(4):477–492
- Oner Z, Dilek Y (2011) Supradetachment basin evolution during continental extension: the Aegean province of western Anatolia, Turkey. *Geol Soc Am Bull* 123:2115–2141. <https://doi.org/10.1130/B30468.1>
- Oner Z, Dilek Y (2013) Fault kinematics in supradetachment basin formation, Menderes core complex of western Turkey. *Tectonophysics* 608:1394–1412
- Ozdemir A, Yasar E, Cevik G (2017) An importance of the geological investigations in Kavaklıdere geothermal field (Turkey). *Geomech Geophys Geo Energy Geo Resour* 3(1):29–49
- Özen T, Bülbül A, Tarcan G (2012) Reservoir and hydrogeochemical characterizations of geothermal fields in Salihli. *Turk J Asian Earth Sci* 60:1–17
- Özgür N (2002) Geochemical signature of the Kizildere geothermal field, western Anatolia, Turkey. *Int Geol Rev* 44:153–163
- Özgür N, Karamenderesi IH (2015) An update of the geothermal potential in the continental rift zone of the Büyük Menderes, Western Anatolia, Turkey. In: Proceedings, fortieth workshop on geothermal reservoir engineering Stanford University, pp 26–28
- Özgür N, Pekdeger A, Wolf M, Stichler W, Seiler KP, Satir M (1998a) Hydrogeochemical and isotope geochemical features of the thermal waters of Kizildere, Salavatli, and Germencik in the rift zone of the Büyük Menderes, western Anatolia, Turkey: preliminary studies. In: Proceedings of 9th international symposium on water-rock interaction, Taupo, New Zealand, vol 30, pp 645–648
- Özgür N, Vogel M, Pekdeger A (1998b) A new type of hydrothermal alteration at the Kizildere geothermal field in the rift zone of the Büyük Menderes, western Anatolia, Turkey
- Özkaymak Ç, Sözbilir H, Uzel B (2013) Neogene–Quaternary evolution of the Manisa Basin: evidence for variation in the stress pattern of the İzmir–Balıkesir Transfer Zone, western Anatolia. *J Geodyn* 65:117–135
- Pfister M, Rybach L, Simsek S (1998) Geothermal reconnaissance of the Marmara Sea region (NW Turkey): surface heat flow density in an area of active continental extension. *Tectonophysics Heat Flow Struct Lithos IV* 291:77–89. [https://doi.org/10.1016/S0040-1951\(98\)00032-8](https://doi.org/10.1016/S0040-1951(98)00032-8)
- Pik R, Marty B (2009) Helium isotopic signature of modern and fossil fluids associated with the Corinth rift fault zone (Greece): implication for fault connectivity in the lower crust. *Chem Geol* 266(1):67–75
- Piomallo C, Morelli A (2003) P wave tomography of the mantle under the Alpine–Mediterranean area. *J Geophys Res Solid Earth*. <https://doi.org/10.1029/2002JB001757>
- Prelević D, Akal C, Foley SF, Romer RL, Stracke A, Van Den Bogaard P (2012) Ultrapotassic mafic rocks as geochemical proxies for post-collisional dynamics of orogenic lithospheric mantle: the case of southwestern Anatolia, Turkey. *J Pet* 53(5):1019–1055
- Purvis M, Robertson A (2005) Sedimentation of the Neogene–Recent Alaşehir (Gediz) continental graben system used to test alternative tectonic models for western (Aegean) Turkey. *Sediment Geol* 173:373–408
- Quilichini A, Siebenaller L, Nachlas WO, Teyssier C, Vennemann TW, Heizler MT, Mulch A (2015) Infiltration of meteoric fluids in an extensional detachment shear zone (Kettle dome, WA, USA): how quartz dynamic recrystallization relates to fluid–rock interaction. *J Struct Geol* 71:71–85
- Reilinger R, McClusky S, Vernant P, Lawrence S, Ergintav S, Cakmak R, Ozener H, Kadirov F, Guliev I, Stepanyan R, Nadariya M, Hahubia G, Mahmoud S, Sakr K, ArRajehi A, Paradissis D, Al-Aydrus A, Prilepin M, Guseva T, Evren E, Dmitrova A, Filikov SV, Gomez F, Al-Ghazzi R, Karam G (2006) GPS constraints on continental deformation in the Africa–Arabia–Eurasia continental collision zone and implications for the dynamics of plate interactions. *J Geophys Res Solid Earth* 111:B05411. <https://doi.org/10.1029/2005JB004051>
- Richardson–Bunbury JM (1996) The Kula volcanic field, western Turkey: the development of a Holocene alkali basalt province and the adjacent normal-faulting graben. *Geol Mag* 133(3):275–283
- Ring U, Gessner K, Gungör T, Passchier CW (1999) The Menderes Massif of western Turkey and the Cycladic Massif in the Aegean—do they really correlate? *J Geol Soc* 156(1):3–6
- Ring U, Johnson C, Hetzel R, Gessner K (2003) Tectonic denudation of a Late Cretaceous–Tertiary collisional belt: regionally symmetric cooling patterns and their relation to extensional faults in the Anatolide belt of western Turkey. *Geol Mag* 140:421–441
- Ring U, Glodny J, Will T, Thomson S (2010) The Hellenic subduction system: high-pressure metamorphism, exhumation, normal faulting, and large-scale extension. *Annu Rev Earth Planet Sci* 38:45–76
- Ring U, Gessner K, Thomson S (2017) Variations in fault-slip data and cooling history reveal corridor of heterogeneous backarc extension in the eastern Aegean Sea region. *Tectonophysics* 700:108–130
- Roche V, Guillou–Frotter L, Jolivet L, Loiselet C, Bouchot V (2015) Subduction and slab tearing dynamics constrained by thermal anomalies in the Anatolia–Aegean region. In: Geophysical research abstracts, vol 17, EGU2015-6882, 2015 EGU General Assembly 2015
- Roche V, Sternai P, Guillou–Frotter L, Jolivet L, Gerya T (2016) Location of eastern Mediterranean hot springs induced by mantle heat flow due to slab roll-back and tearing. In: AGU
- Roche V, Sternai P, Guillou–Frotter L, Menant A, Jolivet L, Bouchot V, Gerya T (2018) Emplacement of metamorphic core complexes and associated geothermal systems controlled by slab dynamics. *Earth Planet Sci Lett* 498:322–333
- Ross HE, Blakely RJ, Zoback MD (2006) Testing the use of aeromagnetic data for the determination of Curie depth in California. *Geophysics* 71(5):L51–L59
- Salaün G, Pedersen HA, Paul A, Farra V, Karabulut H, Hatzfeld D, Papazachos C, Childs DM, Pequegnat C, Team S, others (2012) High-resolution surface wave tomography beneath the Aegean–Anatolia region: constraints on upper-mantle structure. *Geophys J Int* 190:406–420
- Schlinger CM (1985) Magnetization of lower crust and interpretation of regional magnetic anomalies: example from Lofoten and Vesterålen, Norway. *J Geophys Res Solid Earth* 90(B13):11484–11504
- Scholz CH (1980) Shear heating and the state of stress on faults. *J Geophys Res Solid Earth* 85:6174–6184
- Seyitoğlu G (1997) The Simav graben: an example of young EW trending structures in the Late Cenozoic extensional system of western Turkey. *Turk J Earth Sci* 6:135–141
- Seyitoğlu G, Scott BC, Rundle CC (1992) Timing of Cenozoic extensional tectonics in west Turkey. *J Geol Soc* 149(4):533–538
- Seyitoğlu G, Işık V (2015) Late Cenozoic extensional tectonics in western Anatolia: exhumation of the Menderes core complex and formation of related basins. *Bull Miner Res Explor* 151
- Seyitoğlu G, Scott B (1991) Late Cenozoic crustal extension and basin formation in west Turkey. *Geol Mag* 128(2):155–166
- Seyitoğlu G, Tekeli O, Çemen I, Sen S, Işık V (2002) The role of the flexural rotation/rolling hinge model in the tectonic evolution of the Alaşehir graben, western Turkey. *Geol Mag* 139:15–26

- Seyitoğlu G, Işık V, Cemen I (2004) Complete Tertiary exhumation history of the Menderes massif, western Turkey: an alternative working hypothesis. *Terra Nova* 16(6):358–364
- Seyitoğlu G, Işık V, Esat K (2014) A 3D model for the formation of turtleback surfaces: the Horzum Turtleback of western Turkey as a case study. *Turk J Earth Sci* 23(5):479–494
- Seyitoğlu G, Scott BC (1996) The cause of NS extensional tectonics in western Turkey: tectonic escape vs back-arc spreading vs orogenic collapse. *J Geodyn* 22(1–2):145–153
- Sheppard SMF (1977) The Cornubian batholith, SW England: D/H and $^{18}\text{O}/^{16}\text{O}$ studies of kaolinite and other alteration minerals. *J Geol Soc* 133(6):573–591
- Sheppard SM (1981) Stable isotope geochemistry of fluids. *Phys Chem Earth* 13:419–445
- Shimizu A, Sumino H, Nagao K, Notsu K, Mitropoulos P (2005) Variation in noble gas isotopic composition of gas samples from the Aegean arc, Greece. *J Volcanol Geoth Res* 140(4):321–339
- Sibson RH, Moore JMM, Rankin AH (1975) Seismic pumping—a hydrothermal fluid transport mechanism. *J Geol Soc* 131(6):653–659
- Simsek S (1985) Geothermal model of Denizli, Sarayköy-Buldan area. *Geothermics* 14:393–417
- Simsek S (2003) Hydrogeological and isotopic survey of geothermal fields in the Büyük Menderes graben, Turkey. *Geothermics* 32:669–678
- Simsek S, Demir A (1991) Reservoir and cap rock characteristics of some geothermal fields in turkey and encountered problems based on lithology. *J Geotherm Res Soc Jpn* 13:191–204
- Şimşek Ş (1984) Aydın-Germencik-Omerbeyli geothermal field of Turkey. In: Proceeding of UN seminar on utilization of geothermal energy for electric power production and space heating
- Souche A, Medvedev S, Andersen TB, Dabrowski M (2013) Shear heating in extensional detachments: implications for the thermal history of the Devonian basins of W Norway. *Tectonophysics* 608:1073–1085
- Sözbilir H (2001) Extensional tectonics and the geometry of related macroscopic structures: field evidence from the Gediz detachment, western Turkey. *Turk J Earth Sci* 10:51–67
- Spakman W, Wortel R (2004) A tomographic view on Western Mediterranean geodynamics. In: Cavazza W, Roure FM, Spakman W, Stampfli GM, Ziegler PA (eds) *The TRANSMED Atlas—the Mediterranean region from crust to Mantle*. Springer, Berlin, pp 31–52
- Taillefer A, Soliva R, Guillou-Frottier L, Le Goff E, Martin G, Seranne M (2017) Fault-related controls on upward hydrothermal flow: an integrated geological study of the têt fault system, eastern pyrénées (France). *Geofluids* 2017:8190109. <https://doi.org/10.1155/2017/8190109>
- Tarcan G, Gemici Ü (2003) Water geochemistry of the Seferihisar geothermal area, Izmir, Turkey. *J Volcanol Geotherm Res* 126:225–242
- Tarcan G, Filiz S, Gemici U (2000) Geology and geochemistry of the Salihli geothermal fields, Turkey. In: Books proceeding, pp 1829–1834
- Taylor HP (1974) The application of oxygen and hydrogen isotope studies to problems of hydrothermal alteration and ore deposition. *Econ Geol* 69(6):843–883
- Tekin S, Akin S (2011) Estimation of the formation temperature from the inlet and outlet mud temperatures while drilling geothermal formations. In: Proceedings of 36th workshop on geothermal reservoir engineering. Stanford University, Stanford
- Temiz U, Eikenberg J (2011) U/Th dating of the travertine deposited at transfer zone between two normal faults and their neotectonic significance: cambazli fissure ridge travertines (the Gediz Graben-Turkey). *Geodinamica Acta* 24(2):95–105
- Tezcan AK (1995) Geothermal explorations and heat flow in Turkey. *Terr Heat Flow Geotherm Energy Asia* 31:23–42
- Tureyen O, Gulgor A, Erkan B, Satman A (2016) Recent expansions of power plants in Figuris concession in the Germencik geothermal field, Turkey. In: Proceedings
- Ulugergerli EU, Seyitoğlu G, Başokur AT, Kaya C, Dikmen U, Candansayar ME (2007) The geoelectrical structure of northwestern Anatolia, Turkey. *Pure Appl Geophys* 164(5):999–1026
- Vengosh A, Helvacı C, Karamanderesi İH (2002) Geochemical constraints for the origin of thermal waters from western Turkey. *Appl Geochem* 17:163–183
- Wannamaker PE, Hasterok DP, Doerner WM (2006) Possible magmatic input to the Dixie Valley geothermal field, and implications for district-scale resource exploration, inferred from magnetotelluric (MT) resistivity surveying. In: GRC 2006 annual meeting: geothermal resources-securing our energy future
- Wortel MJR, Spakman W (2000) Subduction and slab detachment in the Mediterranean-Carpathian region. *Science* 290:1910–1917
- Yildirim N, Aydogdu O, Sarp S (2005) Constraint problems and solution alternatives for potentially available integrated geothermal energy utilization in Turkey. In: Proceedings of world geothermal congress April 24–29
- Yılmaz Y, Genç ŞC, Güner F, Bozcu M, Yılmaz K, Karacık Z, Altunkaynak Ş, Elmas A (2000) When did the western Anatolian grabens begin to develop? In: Bozkurt E, Winchester JA, Piper JDA (eds) *Tectonics and magmatism in Turkey and the surrounding area*, vol 173. Geological Society Special Publications, London, pp 353–384
- Yılmazer S, Karamanderesi İ (1994) Kuşunlu jeotermal alanının (Salihli-Manisa) jeolojisi ve jeotermal potansiteli. *Dünya Enerji Konseyi Türkiye* 6:17–22
- Yılmazer S, Pasvanoğlu S, Vural S (2010) The relation of geothermal resources with young tectonics in the Gediz graben (West Anatolia, Turkey) and their hydrogeochemical analyses. In: Proceedings world geothermal congress, pp 1–10